

## The Temperature Dependence of the Liquid Water Path of Low Clouds in the Southern Great Plains

ANTHONY D. DEL GENIO

*NASA Goddard Institute for Space Studies, New York, New York*

AUDREY B. WOLF

*Science Systems and Applications, Inc., Institute for Space Studies, New York, New York*

(Manuscript received 19 May 1999, in final form 10 November 1999)

### ABSTRACT

Satellite observations of low-level clouds have challenged the idea that increasing liquid water content with temperature combined with constant physical thickness will lead to a negative cloud optics feedback in a decadal climate change. The reasons for the satellite results are explored using 4 yr of surface remote sensing data from the Atmospheric Radiation Measurement Program Cloud and Radiation Testbed site in the southern Great Plains of the United States. It is found that low-cloud liquid water path is approximately invariant with temperature in winter but decreases strongly with temperature in summer, consistent with satellite inferences at this latitude. This behavior occurs because liquid water content shows no detectable temperature dependence while cloud physical thickness decreases with warming. Thinning of clouds with warming is observed on seasonal, synoptic, and diurnal timescales; it is most obvious in the warm sectors of baroclinic waves. Although cloud top is observed to slightly descend with warming, the primary cause of thinning is the ascent of cloud base due to the reduction in surface relative humidity and the concomitant increase in the lifting condensation level of surface air. Low-cloud liquid water path is not observed to be a continuous function of temperature. Rather, the behavior observed is best explained as a transition in the frequency of occurrence of different boundary layer types. At cold temperatures, a mixture of stratified and convective boundary layers is observed, leading to a broad distribution of liquid water path values, while at warm temperatures, only convective boundary layers with small liquid water paths, some of them decoupled, are observed. Our results, combined with the earlier satellite inferences, suggest a reexamination of the commonly quoted 1.5°C lower limit for the equilibrium global climate sensitivity to a doubling of CO<sub>2</sub>, which is based on models in which liquid water increases with temperature and cloud physical thickness is constant.

### 1. Introduction

Despite the considerable research devoted to understanding the role of clouds in climate change, there have been few observational studies that provide evidence as to even the sense of any component of cloud feedback. Thus, the original estimate that the global sensitivity of climate to a doubling of CO<sub>2</sub> concentration is uncertain to within a range of 1.5°–4.5°C (U.S. National Academy of Sciences 1979) has not been narrowed in more recent assessments (Houghton et al. 1996).

A major contributor to the cited range of uncertainty is the question of how the optical thickness of clouds will respond to a perturbation. Early climate models that assumed fixed optical properties but allowed for variable cloud cover gave sensitivities near or above the upper

end of the range. It was pointed out, though, by Paltridge (1980) and Charlock (1982) that these results might be altered by changes in cloud optical properties. Somerville and Remer (1984) used a one-dimensional radiative-convective model to illustrate that increases in cloud liquid water content with rising temperature could induce a negative feedback that might halve the climate sensitivity. Betts and Harshvardhan (1987) calculated from first principles the temperature dependence of the adiabatic liquid water content of a lifted air parcel and thereby quantified the potential negative optical thickness feedback.

Temperature-dependent optical thickness based on the Betts and Harshvardhan formula has been incorporated into several GCMs with diagnostic cloud schemes, usually resulting in a negative optical thickness feedback similar to that anticipated by Somerville and Remer (cf. Cess et al. 1990). Among the 13 GCMs in the first Atmospheric Model Intercomparison Project that did not prescribe optical thickness, 7 relate it to a liquid water

---

*Corresponding author address:* Dr. Anthony D. Del Genio, NASA GISS, 2880 Broadway, New York, NY 10025.  
E-mail: adelgenio@giss.nasa.gov

content (LWC) that is assumed to increase with temperature at either the adiabatic rate, a fraction thereof, or at a rate determined by the saturation humidity of water vapor, an even more extreme behavior (Phillips 1994). However, GCMs with prognostic cloud water budget approaches to parameterization produce a wide variety of optical thickness feedbacks for several reasons. Senior and Mitchell (1993) predict a negative optical thickness feedback in the U.K. Met. Office GCM, their results being dominated by the approximately adiabatic temperature dependence of liquid water content their model simulates. However, increasing cloud water affects both the albedo and emissivity of clouds. In an early version of the ECHAM GCM (Roeckner 1988), the positive feedback due to the increased greenhouse effect of high clouds in a warmer climate outweighs the negative feedback due to increased albedo of all clouds, giving an overall small positive optical thickness feedback despite approximately adiabatic liquid water behavior in their model. Furthermore, climate changes in sinks of cloud liquid water can sometimes outweigh changes in the condensation source. Li and LeTreut (1992), for example, simulate a strong positive optical thickness feedback in the LMD GCM because, beyond a threshold liquid water content value, water is lost via precipitation, and this happens more readily in the warmer climate. Finally, it must be remembered that liquid water content is only one contributing factor to optical thickness feedback. In general we can write the visible cloud optical thickness  $\tau$  as

$$\tau = 1.5\delta\mu\Delta z/(\rho_w r_e),$$

where  $\mu$  is the liquid water content,  $\Delta z$  the cloud physical thickness,  $\rho_w$  the density of liquid water,  $r_e$  the effective radius of the droplet size distribution, and  $\delta$  a scaling parameter that takes into account the radiative effects of subgrid-scale liquid water inhomogeneity. Climate changes in any of these other parameters might conceivably alter the feedback due to liquid water content changes alone.

Available observational evidence suggests that the behavior of the optical properties of clouds is indeed more complex than the simple behavior of adiabatic liquid water content. The basis for Somerville and Remer's original calculation of negative cloud optics feedback was a compilation of aircraft liquid water estimates made over the former Soviet Union by Feigelson (1978); these showed generally increasing liquid water content with temperature, except for a slight downturn at  $T > 10^\circ\text{C}$ . On the other hand, satellite microwave observations of the North Atlantic by Curry et al. (1990) showed no tendency for vertically integrated liquid water paths to increase with temperature. Tselioudis et al. (1992) and Tselioudis and Rossow (1994) performed a global survey of the temperature dependence of the optical thickness of low clouds in the International Satellite Cloud Climatology Project (ISCCP) dataset. They found that  $\tau$  increases with temperature ( $T$ ) at cold tempera-

tures, especially over land (consistent with Feigelson's liquid water content data), but it decreases with increasing temperature at warm temperatures, especially over the oceans. Greenwald et al. (1995) observed similar behavior in their analysis of Special Sensor Microwave Imager (SSM/I) oceanic cloud liquid water paths.

These results appear to have significant implications for GCM estimates of cloud feedback in a climate change. Tselioudis et al. (1998) show that the Goddard Institute for Space Studies (GISS) GCM at least qualitatively reproduces the latitudinal variation of low cloud  $d\tau/dT$  in the current climate (from positive at high latitudes to negative at lower latitudes) and that this behavior is diagnostic of the low cloud optics feedback in a  $\text{CO}_2$  doubling simulation. The net effect is that low cloud optics feedback decreases the polar amplification of climate warming predicted by all GCMs. Yao and Del Genio (1999) showed that the net global cloud optics feedback in the GCM was slightly positive, because the generally positive feedback from low clouds was largely offset by the negative feedback due to thickening of high cumulus anvil clouds. They pointed out that, given the observational evidence for the temperature dependence of  $\tau$  globally, the Intergovernmental Panel on Climate Change (IPCC, Houghton et al. 1996) estimate of the low end of the range of possible climate sensitivities (unchanged from the original  $1.5^\circ\text{C}$ ) should be increased by at least half a degree.

Satellite data by themselves cannot reveal the physical mechanisms responsible for this peculiar aspect of low cloud behavior. In the GISS GCM, the latitudinal variation in the sign of  $d\tau/dT$  occurs for three different reasons: 1) at high latitudes, the behavior is close to that inferred from the temperature dependence of adiabatic liquid water content; 2) in the subtropics, there is a weak tendency for clouds to thin with warming due to decreasing cloud physical thickness associated with decreasing relative humidity and/or increasing stability; 3) in the tropics, drizzle and entrainment depletion of liquid water tend to make low clouds less opaque with warming. Although plausible, these mechanisms have not been verified as the explanation of the satellite results. One potential source of insights is the climatologies of cloud and atmospheric parameters being acquired by the Department of Energy (DOE) Atmospheric Radiation Measurement Program (ARM) Cloud and Radiation Testbed (CART) sites at three locations, one each in the midlatitudes, Tropics, and polar regions. The midlatitude southern Great Plains (SGP) CART site has been in operation long enough for a climatologically significant dataset to have been processed. In the ISCCP data, land areas at the latitude of the SGP ( $36.6^\circ\text{N}$ ) exhibit low cloud  $d\tau/dT \sim 0$  in winter and  $d\tau/dT < 0$  in summer (see Fig. 2a of Tselioudis and Rossow 1994), so the ARM dataset may provide insights into the causes of the transition from negative to positive cloud optics feedback. In the next section, we describe the data and analysis techniques employed. Section 3 discusses the

basic temperature dependence of liquid water path (LWP) in warm and cold seasons and the factors that contribute to it. Section 4 explores the seasonal differences in low cloud properties and the dependence on baroclinic wave and diurnal phase. Section 5 examines the characteristics of PBL dynamic and thermodynamic structure that cause the observed temperature dependence. The implications of our work for cloud feedback and climate change are discussed in section 6.

## 2. Data and analysis methods

Our approach is to select times at which only low clouds are present over the ARM SGP Central Facility, to mimic the conditions under which the ISCCP results are obtained, to isolate the times when low cloud optical properties have the greatest impact on the planetary radiation balance, and to avoid the ambiguities associated with remote sensing of multiple cloud layers. To perform the analysis, we use four datasets from the SGP Central Facility.

- The Microwave Water Radiometer (MWR) estimates cloud LWP over a 5-min averaging interval. For a typical lower-troposphere wind speed at the SGP of 5–10 m s<sup>-1</sup>, this implies an effective spatial resolution of 1.5–3.0 km, about a factor of 2 better than that of ISCCP.
- The Belfort Laser Ceilometer (BLC) measures cloud-base height ( $z_b$ ) with 30-s time resolution. We average all BLC observations with low cloud present (height 0–3 km) over 5-min intervals that match the MWR LWP averaging interval.
- Geostationary Operational Environmental Satellite (GOES) infrared satellite brightness temperatures at half-hour intervals identify scenes with only low clouds at the SGP Central Facility (cloud-top pressure > 680 mb as determined by comparison with the nearest sounding) and provide a good estimate of the cloud-top temperature of these clouds if their optical thicknesses are sufficiently large (see discussion below). Individual GOES pixels have 4-km resolution. We average cloud-top temperature over the 4 pixels nearest the Central Facility location to account for navigation uncertainties. Scenes in which the maximum and minimum temperatures among the 4 pixels differ by >5 K are interpreted as mixed cloud-type scenes and are excluded from the analysis. MWR data with no satellite image within 15 min are excluded as well.
- The Balloon Borne Sounding System translates cloud-top temperature into cloud-top height ( $z_t$ ), defines a mean cloud temperature, and provides ancillary information such as relative humidity, wind, and pressure for characterizing thermodynamic and synoptic conditions. Soundings are available every 3 h during intensive observation periods (IOP) and 1–5 times per day at other times. Cloud observations are matched

to the nearest sounding in time, but we exclude cloud data for which no soundings exist within 3 h. This is probably adequate to capture the important scales of temperature variability but may not always be adequate for humidity variations.

From these basic parameters, we derive cloud physical thickness  $\Delta z = z_t - z_b$  and cloud liquid water content  $LWC = LWP/\Delta z$ . Unfortunately, at the time of this analysis cloud optical thickness and droplet effective radius products were not yet being routinely produced from the ARM data streams, so they will not be discussed here. Using the BLC to detect clear skies and compiling histograms of MWR LWP retrievals at such times (Fig. 1), we estimate the accuracy of the instrument and retrieval algorithm to be approximately  $\pm 0.04$  mm, similar to that estimated for satellite microwave LWP algorithms (Lin and Rossow 1994). LWP values < 0.04 mm are therefore excluded from the analysis, which eliminates some actual detections of thinner clouds by the MWR but also guarantees that LWP values for the clouds that remain have  $< O(1)$  errors. For typical droplet size distributions, this then restricts us to optical thicknesses  $\tau \geq 5$ . We also exclude LWP values > 1 mm, which imply an unrealistically large low cloud optical depth ( $\tau \geq 75$ –100) for plausible droplet sizes. Note also in Fig. 1 that the MWR LWP algorithm is slightly negatively biased in cold conditions ( $-0.01$  mm) and slightly positively biased ( $+0.02$  mm) in warm conditions. Finally, in addition to the quality control screening performed by the ARM project, we visually inspect soundings and satellite imagery with unusual behavior and reject those with obvious errors (usually due to missing data).

ISCCP DX retrievals for the First ISCCP Regional Experiment (FIRE) II IOP period in nearby Coffeyville, Kansas, show that for low clouds with  $\tau > 5$ , cloud-top and infrared (IR) brightness temperatures never differ by more than a few kelvins (Fig. 2), resulting in a cloud-top altitude error of several hundred meters or less. The temperature bias is negative and largest at the highest temperatures, suggesting that the brightness temperature slightly overestimates cloud-top height due to weak absorption by water vapor. The sign of the bias, if corrected, only reinforces the conclusions about temperature dependence of cloud physical thickness we present later.

For this study we have analyzed all ARM SGP data for the period July 1994–June 1997. Months in which all four instrument data streams were not available are excluded, as are months with infrequent occurrence of isolated low cloud (typically drought periods with little cloudiness of any kind or convectively disturbed periods with frequent obscuration by middle and high cloud). Transition season months are also eliminated to allow us to focus on differences between the behavior of low clouds in colder and warmer climate regimes. The remaining 18 months of data (comprising 3394 individual

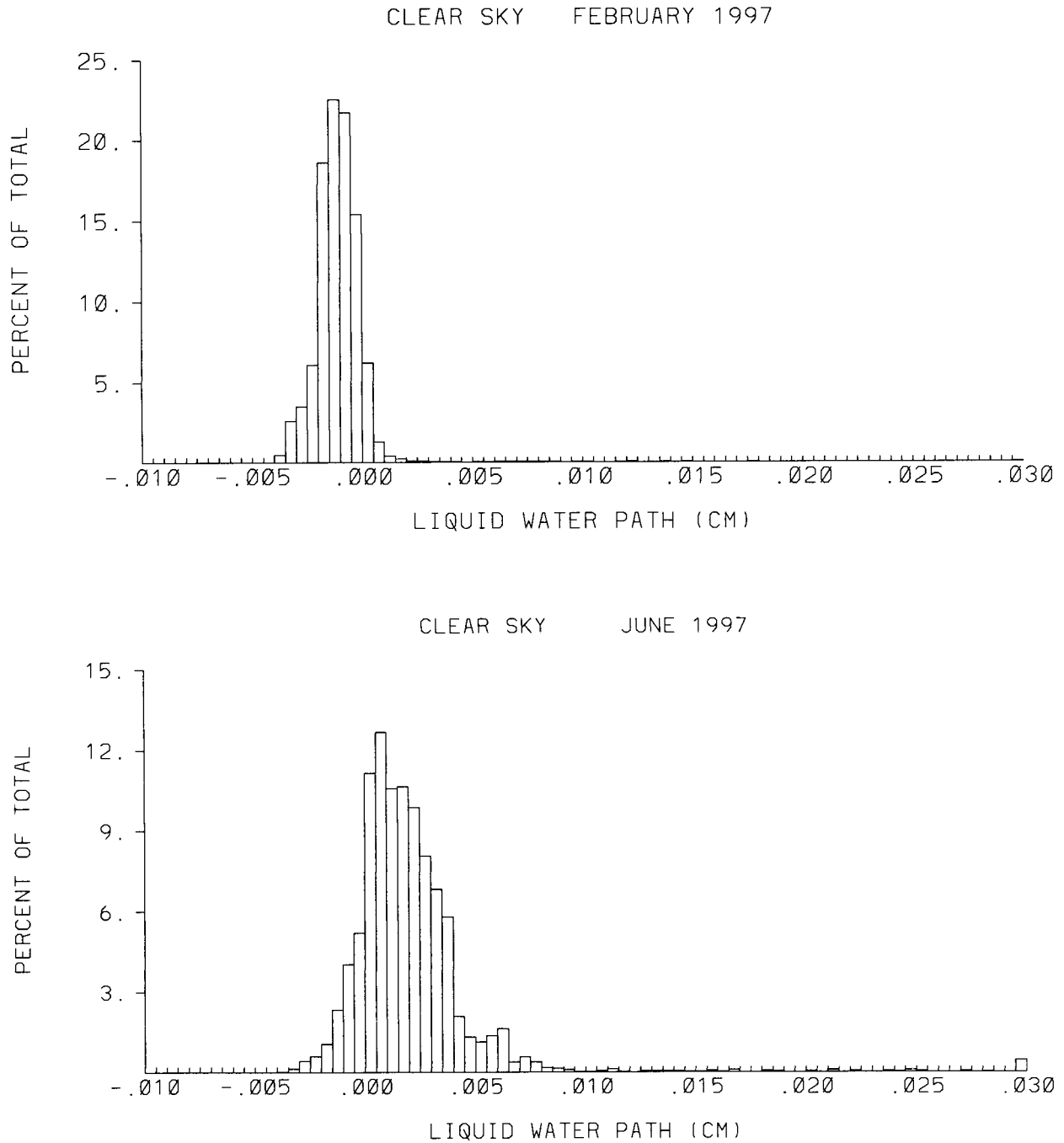


FIG. 1. Examples of frequency distributions of MWR LWP retrievals for all 5-min intervals over which the BLC detected completely clear skies during (top) Feb 1997 and (bottom) Jun 1997. The LWP bias (standard deviation) magnitudes are  $-0.010$  ( $0.014$  mm) for Feb and  $0.021$  ( $0.034$  mm) for Jun.

low cloud observations and 211 atmospheric soundings) are divided into “warm season” (1773 cloud observations, 127 soundings) and “cold season” (1621 cloud observations, 84 soundings) ensembles (Table 1).

It is difficult to isolate the true temperature dependence of any climate parameter in observations because much of the observed variability is due to dynamics.

Furthermore, temperature dependence on one timescale does not necessarily imply a similar temperature dependence on other timescales. In the midlatitudes, synoptic timescale variability is dominated by the passage of baroclinic waves, while diurnal variability is large in continental regions and nonnegligible seasonal variation occurs even within one of the ensembles. Thus, for each

FIRE II Central US  
33N-40N, 105W-85W  
911107-911116  
(1314 pts)  
(Opt. Depth > 5.0)

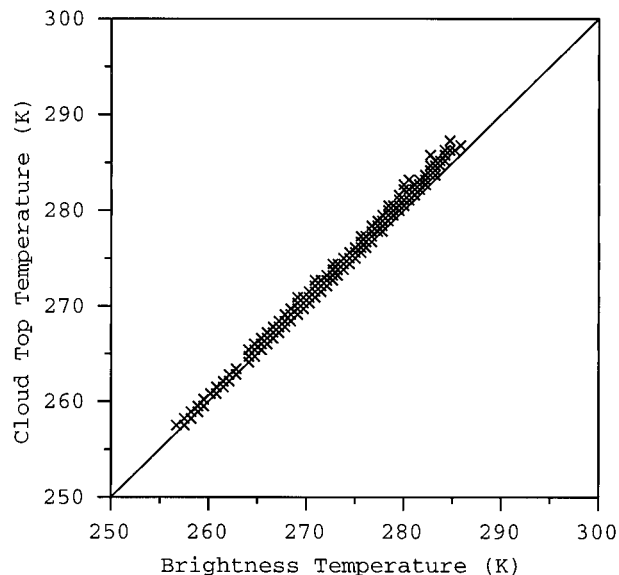


FIG. 2. ISCCP DX retrieved cloud-top temperature vs input IR brightness temperature for all low clouds with  $\tau > 5$  observed during the Nov 1991 FIRE II IOP period in Coffeyville, Kansas.

ensemble we calculate a climatological diurnal cycle and seasonal variation of temperature, zonal wind, and meridional wind (including all soundings for the months in our ensembles, not only those with isolated low cloud). These are subtracted from the original measurements to define positive and negative instantaneous deviations from the norm ( $T'$ ,  $u'$ ,  $v'$ , respectively). The signs of  $v'$  and  $T'$  are then used to define a crude synoptic classification of the data as follows.

- $v' > 0$ ,  $T' > 0$ : identified as the warm sector between warm and cold fronts; characterized by warm advection from the south and west, generally westerly wind anomalies (mean  $u' = +1.6/+2.6$  m s<sup>-1</sup> in cold/warm seasons, respectively) and falling or nearly steady surface pressure ( $dp_s/dt = -0.15/+0.02$  mb h<sup>-1</sup>) as the surface low approaches and passes to the north.
- $v' < 0$ ,  $T' < 0$ : identified with the subsidence region behind the cold front and the wraparound region to the north/northwest of the surface low; characterized by cold advection from the north, easterly wind anomalies ( $u' = -3.3/-1.2$  m s<sup>-1</sup>), and steady or rising surface pressure near and after surface low passage ( $dp_s/dt = +0.39/-0.02$  mb h<sup>-1</sup>).
- $v' > 0$ ,  $T' < 0$ : identified with the pre-warm frontal region in advance of the surface low; characterized by anomalous cold advection northeast of a passing low, easterly wind anomalies ( $u' = -2.3/-0.1$  m s<sup>-1</sup>)

TABLE 1. Months included in the cold season and warm season ensembles of SGP observations analyzed in this paper.

Cold season	Warm season
Dec 1994	Jul 1994
Jan 1995	Sep 1994
Feb 1995	Jun 1995
Mar 1996	Jul 1995
Dec 1996	Sep 1995
Jan 1997	Jun 1996
Feb 1997	Jul 1996
Mar 1997	Aug 1996
	Sep 1996
	Jun 1997

and rapidly falling pressure ( $dp_s/dt = -0.22/-0.20$  mb h<sup>-1</sup>).

- $v' < 0$ ,  $T' > 0$ : identified with a building ridge; characterized by anomalous warm advection southeast of a surface high, easterly wind anomalies ( $u' = -3.4/-3.0$  m s<sup>-1</sup>), and rapidly rising surface pressure ( $dp_s/dt = +0.49/+0.25$  mb h<sup>-1</sup>).

Undoubtedly this classification scheme is not perfect, but it allows us to get an idea of the climatological effect of baroclinic waves on low cloud properties while avoiding the necessity of visually inspecting 18 months of weather maps. The classifications are qualitatively consistent with regions of prevalent low clouds in the baroclinic wave composites of Lau and Crane (1995). The segmentation of the data described above allows us to isolate three timescales: seasonal temperature effects on low clouds within a given baroclinic wave segment, synoptic variations due to the dynamics itself, and effects due to diurnal temperature variations.

### 3. Temperature dependence of low cloud properties

Figure 3 shows LWP as a function of mean cloud temperature for the warm and cold season ensembles. Temperature is only one of the factors affecting cloud properties in a dynamic atmosphere. Furthermore, as described above, observation times for individual instruments at the SGP are not always exactly coincident, and each instrument has a nonnegligible retrieval uncertainty for the parameters used here. These combine to produce considerable scatter in any regression, and only a small fraction of the total variance (15%–25%) of any quantity is explained by its temperature dependence. Nonetheless, the data are clearly consistent with ISCCP optical thickness results of Tselioudis and Rossow (1994). In the warm season, when  $T > 280$  K, low cloud LWP tends to decrease with warming, being highly variable at colder temperatures but almost always small when temperatures are warm, with the transition occurring between 285–290 K. Defining  $f(A) = A^{-1} dA/dT$  for any parameter  $A$ , we find  $f(\text{LWP}) = -0.08$  K<sup>-1</sup> for  $T > 280$  K with a correlation coefficient  $r = -0.39$  for a logarithmic fit ( $r = 0.06$  is significant at

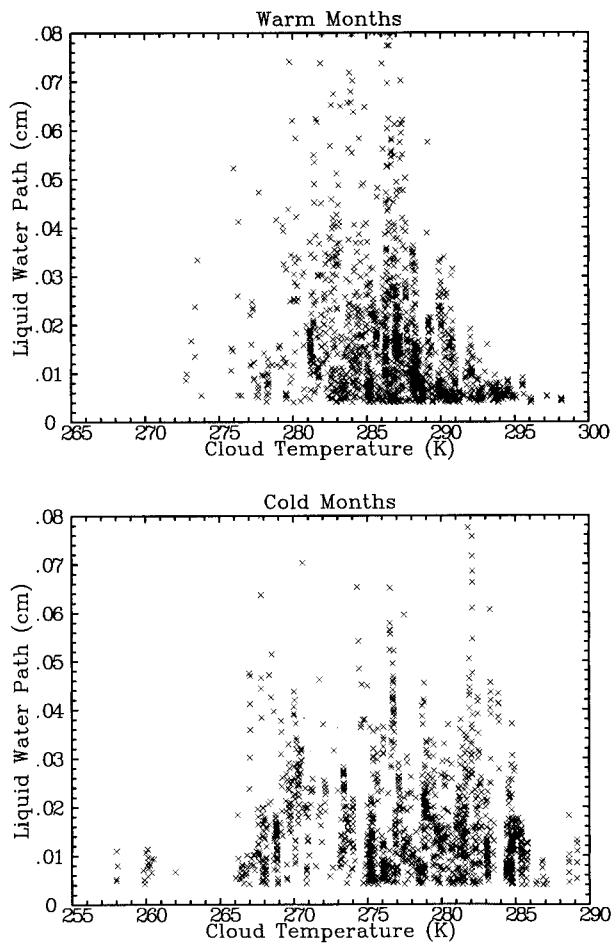


FIG. 3. LWP vs mean cloud temperature for the (top) warm season and (bottom) cold season ensembles at the SGP.

the 99% level). By comparison, Tselioudis and Rossow find  $f(\tau) = -0.05 \text{ K}^{-1}$ , respectively, for all summer midlatitude land points at the same latitude as the SGP.

In the cold season, on the other hand, LWP is only marginally correlated with  $T$  [ $f(\text{LWP}) = -0.01 \text{ K}^{-1}$ ,  $r = -0.11$  for  $T > 265 \text{ K}$ ], but with a slight hint of decreasing LWP for the few points with  $T > 285 \text{ K}$ . This is also consistent with Tselioudis and Rossow's value  $f(\tau) \sim 0$  for the winter season at midlatitude land locations. In both warm and cold seasons LWP appears to increase somewhat with  $T$  for temperatures near and below freezing. This may either be an indication of behavior closer to that of adiabatic liquid water content or a measurement bias due to increasing occurrence of ice, which is not sensed by the MWR, in colder environments.

Figure 4 shows the individual contributions to the temperature dependence of LWP for the warm season ensemble. (Note that we plot LWC vs mean cloud temperature, since it is the local thermodynamic conditions that are relevant to the adiabatic liquid water content of a cloud. On the other hand, correlations between cloud

boundary locations and cloud temperature occur as the cloud moves up or down, which may have nothing to do with the intrinsic temperature dependence we seek; we therefore plot these parameters as a function of surface temperature instead.) LWC is uncorrelated with  $T$  [ $f(\text{LWC}) = -0.01 \text{ K}^{-1}$ ,  $r = -0.04$ ]. Though it is admittedly a noisy field since it is calculated as the ratio of two other cloud parameters, there is certainly no indication of anything like adiabatic behavior. On the other hand, cloud  $\Delta z$  shows a clear tendency to decrease with temperature, that is, low clouds physically thin with warming, at a rate that explains virtually all of the temperature dependence of the independently measured LWP [ $f(\Delta z) = -0.07 \text{ K}^{-1}$ ,  $r = -0.50$ ]. In turn, clouds thin mostly because cloud bases rise with warming [ $f(z_b) = +0.04 \text{ K}^{-1}$ ,  $r = +0.27$ ] but also because cloud tops slightly descend with warming [ $f(z_t) = -0.02 \text{ K}^{-1}$ ,  $r = -0.34$ ].

The temperature dependence of cloud-base height is easily explained. Figure 5 shows that despite the fact that rising parcels that form clouds can originate anywhere in the planetary boundary layer (PBL), observed cloud bases are fairly well predicted (within about 500 m for most points) by the lifting condensation level (LCL) of surface air for the nearest sounding, consistent with expectations for a convective PBL. [The BLC signal apparently slightly penetrates into the cloud and biases cloud base upward. In Figure 5 we have thus shifted cloud base downward based on Micropulse Lidar comparisons with the BLC according to  $z_{\text{MPL}} = 0.013 + 0.84z_{\text{BLC}}$  (D. Han and R. Ellingson 1998, personal communication). This slightly improves agreement but is a small effect.] In turn, the LCL is observed to rise with increasing surface temperature because the relative humidity (RH) of surface air decreases with surface temperature. RH decreases with  $T$  strictly because of the temperature dependence of saturation vapor pressure; surface specific humidities are actually about 50% higher at the warmer times than at the colder times in Fig. 5. Thus, the processes that supply water vapor to the SGP increasingly cannot compete with small- or large-scale dynamical processes that deplete it as temperature rises.

Figure 6 shows the corresponding contributions to the temperature dependence of LWP in the cold season ensemble. As in the warm season, LWC is virtually uncorrelated with  $T$  [ $f(\text{LWC}) = -0.01 \text{ K}^{-1}$ ,  $r = -0.10$ ], so in neither season do we see evidence of adiabatic behavior in above-freezing conditions. Unlike the warm season, cold season cloud bases do not rise [ $f(z_b) = -0.01 \text{ K}^{-1}$ ,  $r = -0.08$ ] or tops descend [ $f(z_t) = -0.005 \text{ K}^{-1}$ ,  $r = -0.13$ ] with warming, accounting for the absence of any observable temperature dependence of LWP.

The reason for the failure of LWC to behave adiabatically in either season is difficult to diagnose from the available observations. Increasing depletion by drizzle with warming does not seem likely, since no rain was recorded at the surface within 30 min of any of the

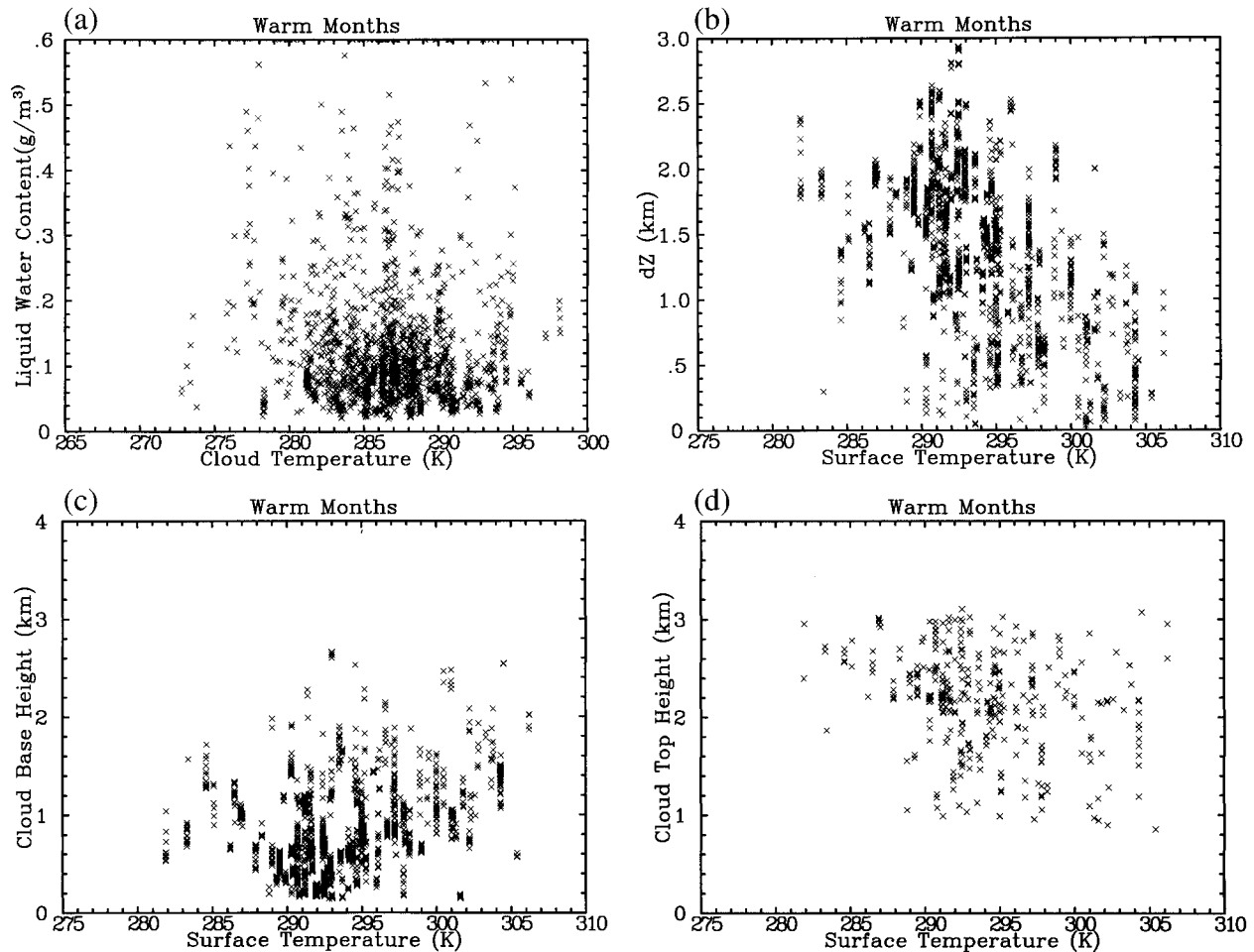


FIG. 4. Temperature dependence of low cloud properties for the warm season ensemble. (a) LWC vs cloud temperature. (b) Cloud physical thickness vs surface temperature. (c) Cloud-base height vs surface temperature. (d) Cloud-top height vs surface temperature.

1773 warm season low cloud observations and was detected for only a few of the cold season cases. This does not rule out the possibility of drizzle that evaporates completely below cloud base, although in general we might expect this to be a less important sink of LWC for continental low clouds with small droplet sizes than for marine stratus, stratocumulus, and trade cumulus.

The other alternative is increased entrainment drying, for which no estimates exist in the absence of cloud turbulence data. Low clouds are often topped by a stabilizing inversion, whose strength can be characterized by the increase or "jump" in virtual dry static energy across the cloud-top interface. As clear air parcels are entrained into the cloud, liquid water evaporates and the resulting cooling reduces parcel buoyancy. If the air above the cloud is sufficiently dry and the temperature inversion weak or nonexistent, that is, if the virtual dry static energy jump is less than some critical value, entrained air will be negatively buoyant and unstable, perhaps promoting further entrainment. The actual jump relative to the critical value can be expressed in terms

of the ratio  $k$  of the cloud-top jumps in moist static energy and latent heat content (vapor plus liquid). The value of  $k$  required for instability depends on the model of cloud mixing used. The value  $k = 0.23$  was suggested by Randall (1980) and Deardorff (1980) as a threshold for instability; a more restrictive limit of  $k = 0.70$  is advocated by MacVean and Mason (1990) using a different model. At the SGP there is considerable scatter in  $k$  (Fig. 7), some of it no doubt due to combined measurement errors from individual instruments and the difficulty in measuring gradients, but there may be a weak tendency for  $k$  to increase with temperature in both warm and cold seasons. Relatively few points exceed the MacVean–Mason instability criterion, but a significant number do exceed the Randall–Deardorff value, particularly in the warm season. Whether this indicates gradually increasing entrainment strength with warming, even in the absence of a catastrophic transition in cloud regime, is not known. Even if entrainment strength is constant, though, entrainment depletion of LWC may still increase with warming if RH above cloud

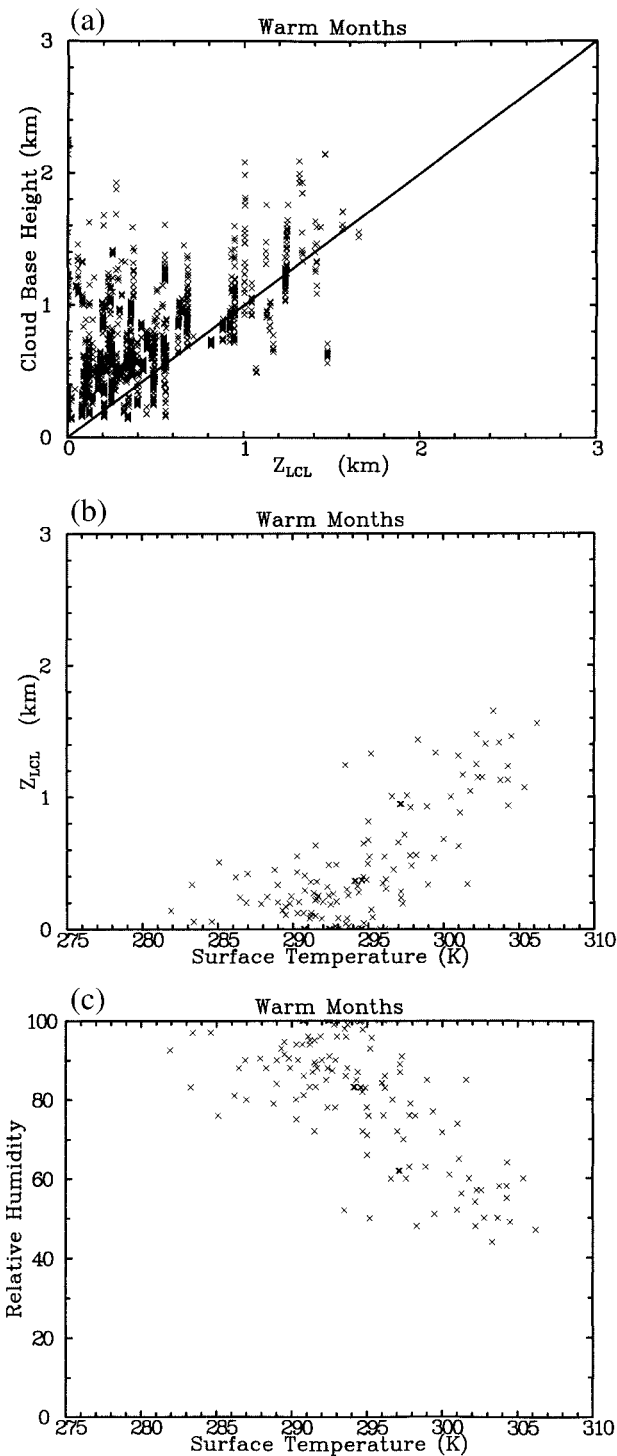


FIG. 5. (a) Observed low cloud-base heights, corrected using MPL data, vs the LCL of surface air. (b) LCL vs surface temperature for low cloud soundings. (c) Surface RH vs surface temperature for low cloud soundings.

top decreases with  $T$ . This appears to be the case, as we will show in section 5.

The observed decrease in cloud-top height with warming, especially in the warm season, might also be explained by increased entrainment erosion of cloud top, although entrainment can conceivably lift cloud top as well (Randall 1984). Large-scale vertical advection does not appear to be the cause; vertical velocity is not measured at the SGP, but neither pressure nor pressure tendency vary systematically with temperature in our data. Horizontal advection of dry air near cloud top cannot be ruled out as a contributor, however.

#### 4. Seasonal, synoptic, and diurnal low cloud variability

The results presented in the previous section are due to variability on several different timescales and a combination of dynamics-related variability and true temperature dependence. To separate these, we composite observations by season, synoptic classification, and diurnal cycle phase. Table 2 shows the mean cloud parameters for each seasonal ensemble and  $v'$ ,  $T'$  category. Isolated low clouds occur in winter preferentially when the weather is warmer than normal and in summer when it is cooler than normal. Averaged over all observations, LWP at the SGP is season-independent, but this hides significant variations with synoptic phase. Under warmer than normal conditions, that is, in the warm sector ( $v' > 0$ ,  $T' > 0$ ) and building high pressure ( $v' < 0$ ,  $T' > 0$ ) regions of baroclinic waves, LWP decreases dramatically from the cold to the warm season. This difference may even be greater, considering the negative/positive bias in LWP in the cold/warm season suggested by Fig. 1. In colder than normal conditions associated with the pre-warm frontal ( $v' > 0$ ,  $T' < 0$ ) and cold sector/wraparound ( $v' < 0$ ,  $T' < 0$ ) regions, however, LWP slightly increases or remains constant from winter to summer instead. In the warm sector region where the clearest seasonal decrease in LWP is observed,  $\Delta z$  also decreases sharply from winter to summer, primarily due to rising cloud base. LWC varies little seasonally in the  $T' > 0$  regions but increases noticeably from winter to summer in the  $T' < 0$  regions.

Figures 8–10 display histograms of the surface remote sensing data used to construct some of the averages in Table 2. The LWP distribution (Fig. 8) in the warm sector region is clearly broader in the cold season relative to the warm season, in which the vast majority of clouds have  $LWP < 0.01$  cm; LWP distributions in the other synoptic regimes do not differ significantly with season or with each other. Cloud-base heights (Fig. 9), which account for most of the seasonal change in  $\Delta z$ , have a noisier distribution for this sample size, but the tendency for much higher cloud bases in summer in the warm sector is still obvious. The summer – winter differences in LWP and  $z_b$ , measured independently by different instruments, combine to produce LWC histograms that are almost identical

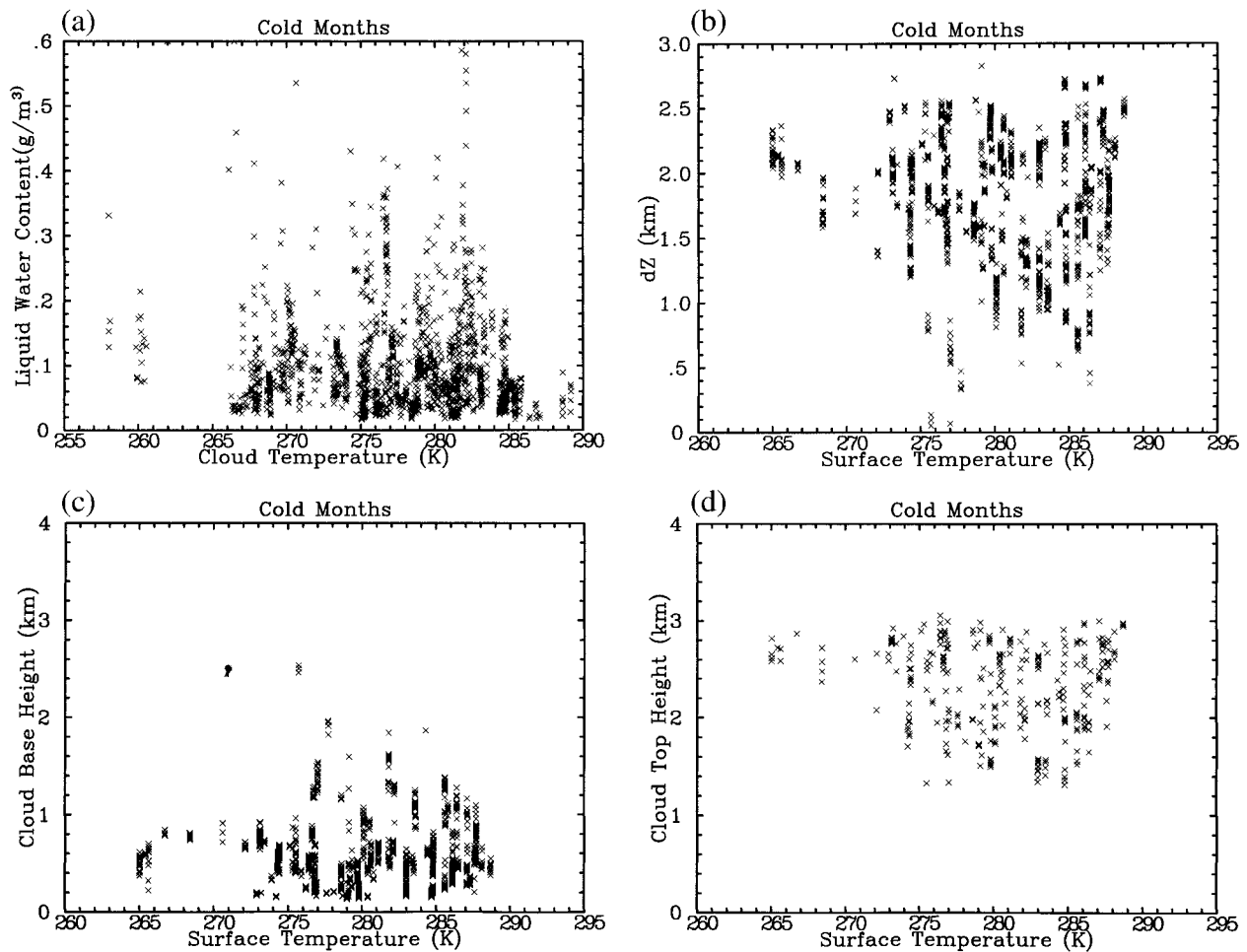


FIG. 6. As in Fig. 4 but for the cold season ensemble.

in the warm sector in the different seasons (Fig. 10). LWC occurrence in the two  $T' < 0$  synoptic categories tends to be shifted toward higher values in the warm season, suggesting that these are the places to expect near-adiabatic low cloud behavior. Cloud-top height and physical thickness histograms (not shown) are sparser and thus extremely noisy because they are constructed using satellite data that are available only every half hour rather than every 5 min, and because they are averaged over an  $8 \text{ km} \times 8 \text{ km}$  area. Despite this, warm sector seasonal population differences in  $\Delta z$  consistent with Table 2 are clearly visible.

Since the mean seasonal and diurnal cycles of surface temperature are removed to define the  $v'$ ,  $T'$  categories, low cloud parameter variations due purely to synoptic-timescale variations can be isolated. Figure 11 shows the synoptic-timescale dependence of LWP and  $\Delta z$  variations on temperature deviations from the mean, binned and averaged in 1 K increments. There are no summer observations for large positive temperature anomalies ( $T' > 5 \text{ K}$ ), because these are typically either convectively disturbed or clear, dry environments in which isolated low cloud is absent. Both LWP and  $\Delta z$  tend to

decrease with instantaneous warming during summer, when the mean temperature is warm, but no synoptic-timescale temperature dependence is obvious during the cold season. Cloud parameters and temperatures can also be composited by diurnal cycle phase (Fig. 12). We see that over the daily temperature range, clouds still tend to be thinnest at times of day when surface temperature is high (afternoon), in both warm and cold seasons. However, no obvious diurnal cycle of low cloud LWP is observed, suggesting that different physics may operate on the diurnal timescale.

### 5. Effects of PBL structure on low cloud properties

Perhaps more than other cloud types, low-level clouds depend on details of the local thermodynamic structure and the degree of small-scale turbulence and coupling to the surface. This is difficult to diagnose systematically at the SGP, given the limited number of soundings taken and the time separation between many of our cloud observations and the nearest sounding. However,

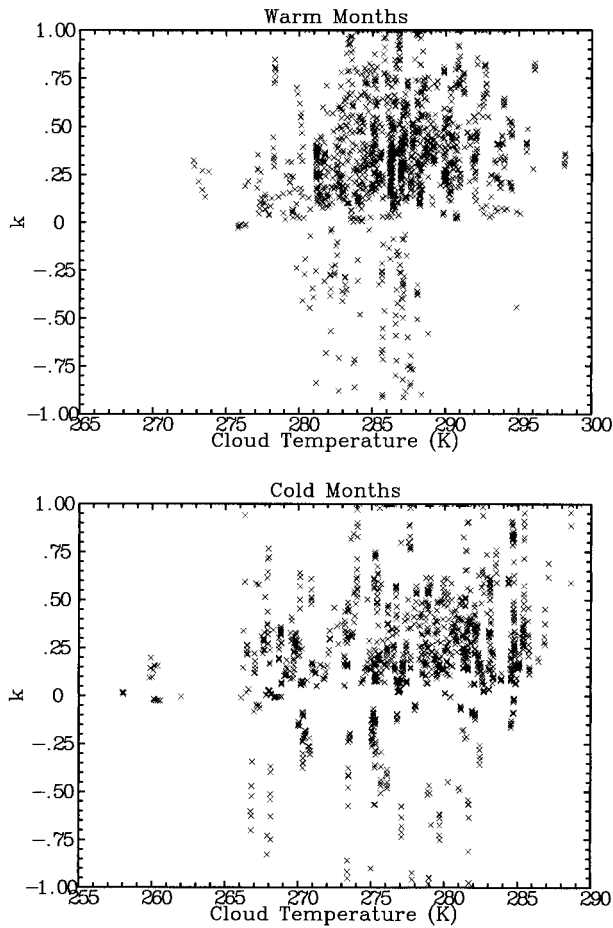


FIG. 7. Cloud-top entrainment jump parameter  $k$  vs cloud temperature for the (top) warm season and (bottom) cold season ensembles.

even the sparse sample available is sufficient to suggest some characteristic differences between low clouds under warmer and cooler surface conditions. Also, given the relative paucity of analyses of continental low clouds relative to their maritime counterparts, it is worthwhile to document the similarities and differences in their occurrence and behavior.

Figures 13 and 14 contrast the cold season and warm season vertical profiles of potential temperature ( $\theta$ ), water vapor mixing ratio ( $q$ ), and RH for the four synoptic categories. Following Albrecht et al. (1995), we define a dimensionless depth of each sounding by normalizing by the mean cloud-top height, that is,  $z' = z/z_c$  (Albrecht et al. used inversion height instead), at times near that of the sounding to clarify the relationship between cloud and PBL structure. Table 2 can be used to convert these to approximate absolute altitudes. In the cold season (Fig. 13), the top of the PBL appears to be near  $z' \sim 0.5$ , based on the local maximum in static stability there and more so by the convergence of  $q$  profiles and sharp decrease in RH for all four synoptic categories above this level. Cloud bases are then typically near or just

TABLE 2. Mean values of low cloud parameters averaged over synoptic category for each of the seasonal ensembles.

	No. of obs clouds/ soundings	LWP (mm)	$z_b$ (m)	$z_r$ (m)	$\Delta z$ (m)	LWC ( $\text{g m}^{-3}$ )
$v' > 0, T' > 0$						
Warm	231/21	0.10	1123	2265	1142	0.11
Cold	719/32	0.15	437	2209	1772	0.10
$v' < 0, T' > 0$						
Warm	262/16	0.16	670	2216	1546	0.12
Cold	263/15	0.19	624	2165	1541	0.13
$v' > 0, T' < 0$						
Warm	471/35	0.19	680	2047	1366	0.15
Cold	224/18	0.15	599	2555	1956	0.08
$v' < 0, T' < 0$						
Warm	809/55	0.16	801	2283	1482	0.14
Cold	415/19	0.16	622	2555	1932	0.09
$T' > 0$						
Warm	493/37	0.13	882	2239	1356	0.12
Cold	982/47	0.16	487	2197	1710	0.11
$T' < 0$						
Warm	1280/90	0.17	756	2196	1440	0.14
Cold	639/37	0.16	614	2555	1941	0.08
All						
Warm	1773/127	0.16	791	2208	1417	0.14
Cold	1621/84	0.16	537	2338	1801	0.10

below the base of the inversion. Above cloud top, static stabilities are similar for all synoptic categories. Within the PBL, there is a clear separation in  $q$  between warmer and colder than normal conditions, with the colder sectors having about 50% the water vapor amount of the warmer sectors and a humidity inversion near the PBL top. There is a hint of a mixed layer within the first 500 m above ground in the northerly flow categories, especially the postfrontal cold sector; this may be a weaker continental analog of the well-defined cold air outbreak regions off the east coasts of continents in which advection of cold air over a warm ocean surface generates fields of shallow cumulus.

The warm season vertical structures (Fig. 14) behave somewhat differently. The inversion level is 100–200 m higher than in the cold season, there is no hint of a mixed layer in the mean for any synoptic category, and the lapse rate above cloud top is decidedly less stable in the warm sector than in the other sectors. Mixing ratios within the PBL group more closely by meridional flow direction than by temperature anomaly, that is, summer PBL humidity at the SGP is controlled by horizontal moisture advection rather than by local thermodynamics. Above the PBL, pre-warm frontal humidities are systematically higher than in the other categories, perhaps a signature of soundings taken through elevated portions of the front. Finally, RH profiles are similar within the PBL but diverge above it, with the free troposphere above the warmer sectors systemati-

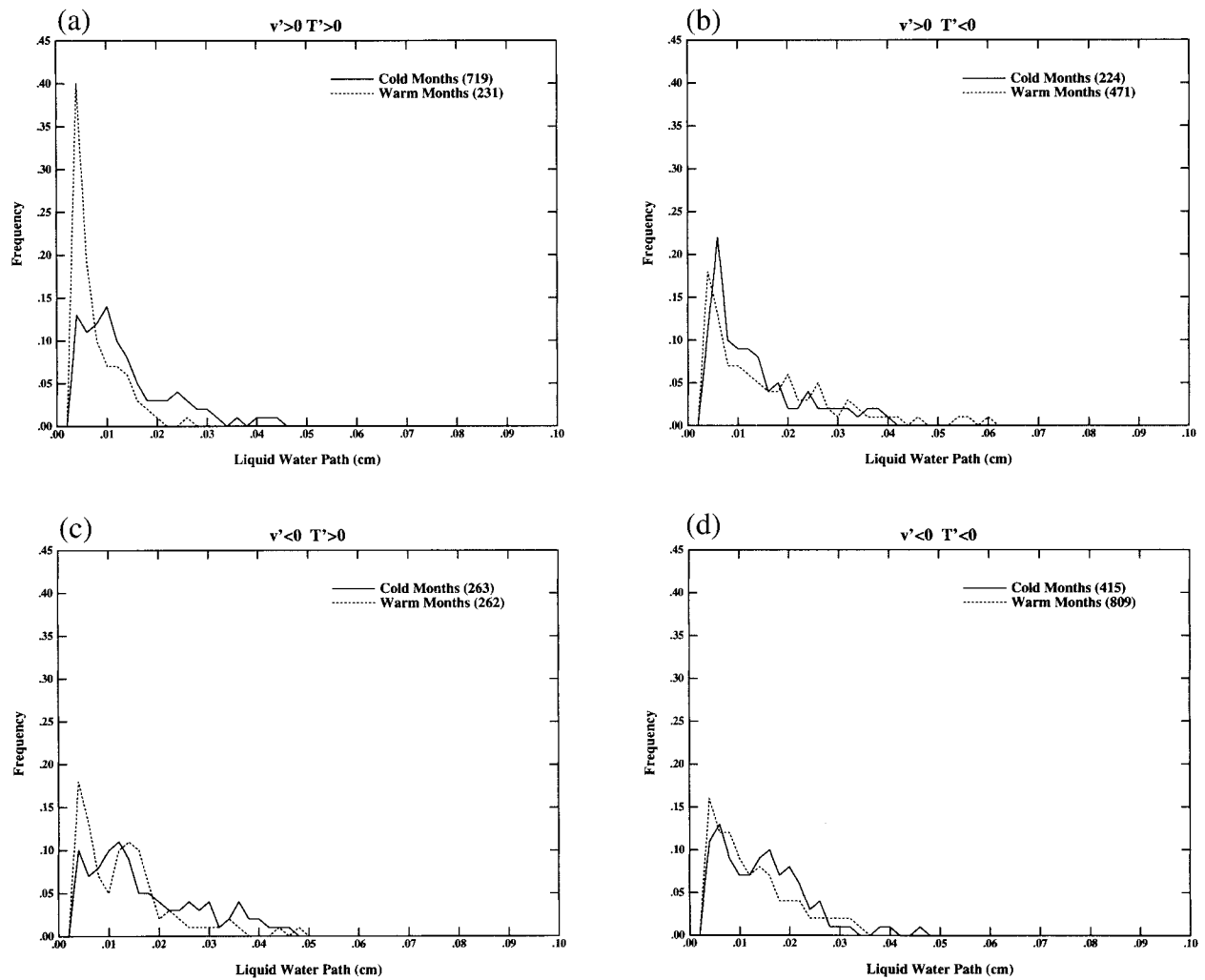


FIG. 8. Frequency distributions of LWP for the warm season (dotted) and cold season (solid) ensembles for the four synoptic categories. The numbers in parentheses in the legends indicate the number of observations in each histogram.

cally drier than that above the colder sectors under isolated low cloud conditions.

A clearer picture of how vertical structure differences may lead to the observed temperature dependence of continental low cloud LWP and optical depth can be obtained by compositing soundings by surface temperature for the warm season (Fig. 15), in which clouds are seen to thin with warming. The colder soundings are quite stable throughout the lower troposphere, while the warmer soundings clearly indicate a convective PBL in the lowest  $\sim 800$  m above ground. The cold PBLs are fairly uniformly moist in RH down to the ground (though dry in  $q$ ) and maintain fairly high RH up to 1200-m altitude, while the warm PBLs exhibit dry surface RH but sharply increasing RH up to the inversion and sharply decreasing RH above, a characteristic signature of a convective cloud-topped boundary layer. This difference in structure is entirely consistent with the larger (smaller) cloud thicknesses observed at cool

(warm) temperatures. Fewer than half the soundings used to produce Fig. 15 have coincident World Meteorological Organization surface-observer cloud classifications available, but those that do show a clear distinction between the cold and warm subsets: 5 of 7 in the cold subset were classified as bad-weather stratus, with a mean cloud cover of 79%, while 7 of 9 in the warm subset were classified as stratocumulus, cumulus, or cumulus-under-stratocumulus, with a mean cloud cover of 49%.

Further insight can be gained, albeit somewhat anecdotally, by examining individual soundings. We can define three broad categories of low-level soundings at the SGP under conditions of isolated low cloud: 1) *Well-mixed* convective PBLs with high but fairly uniform  $q$  up to an inversion level and a rapid transition to dry conditions above; 2) *Decoupled* convective PBLs with multiple well-mixed layers separated by small  $q$  discontinuities below the main inversion level; 3) *Strat-*

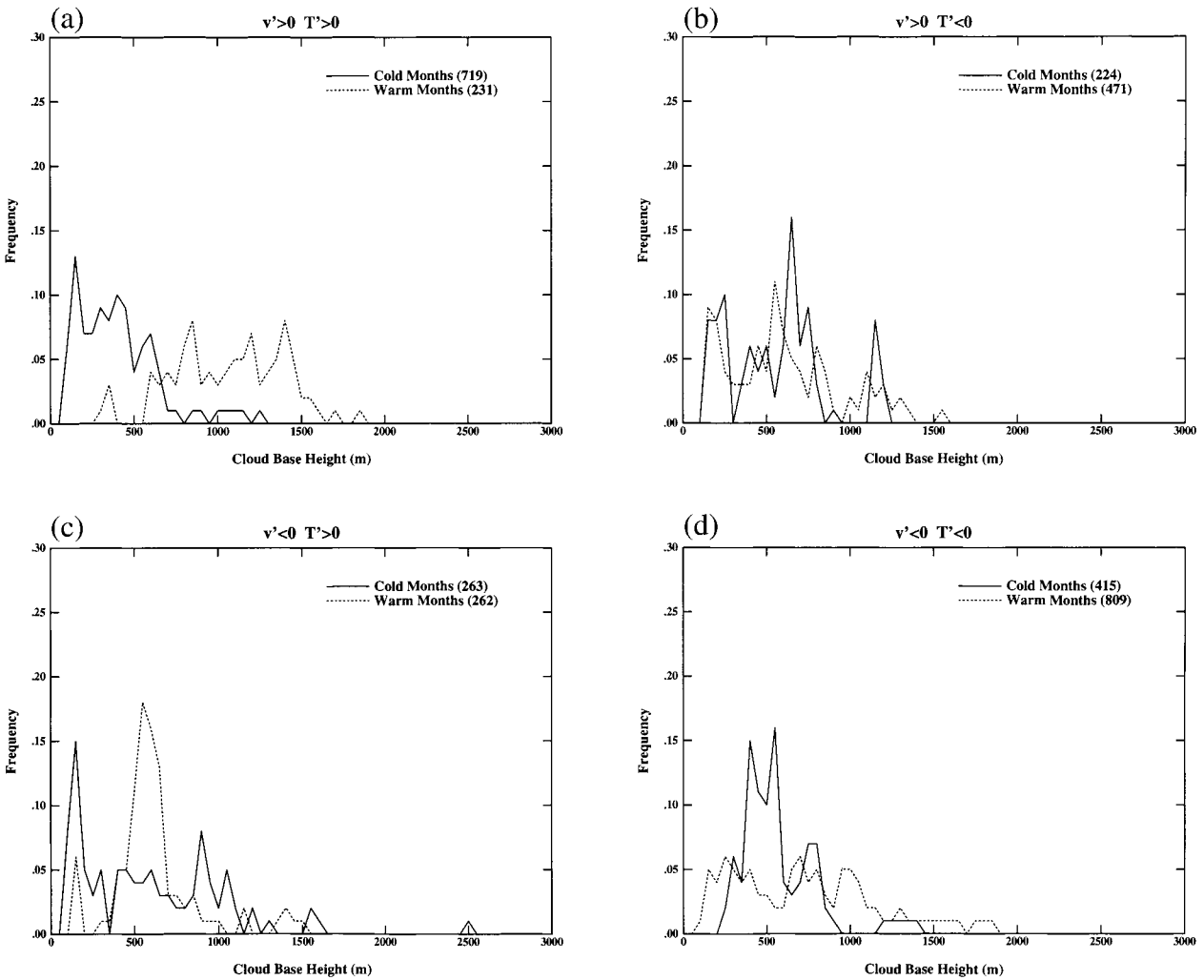


FIG. 9. As in Fig. 8 but for cloud-base height.

ified nonconvective PBLs with large and sometimes complex vertical gradients in  $q$ , indicative of isolated dry and moist layers, some with no evidence of an inversion separating moist near-surface and dry free-troposphere air. Figure 16 shows an example of each type of PBL. For the well-mixed profile, observed cloud base is close to both the LCL and level of free convection (LFC) of surface air and near-inversion base. For the decoupled PBL case, the LCL is near the base of the decoupled layer but observed cloud base is some 500 m higher, near the LFC for lifted air with the moist static energy value of the decoupled layer. For the stratified sounding, on the other hand, LCL is close to the ground but observed cloud base is much higher, suggesting an absence of vertical mixing. For the warm season, warm sector population of 21 soundings, visual inspection suggests that the 9 warmest soundings (all with  $T_s > 300$  K) consisted of 4 well-mixed, 5 decoupled, and 0 stratified PBLs, while the 9 coldest soundings (all with  $T_s \leq 296$  K) contained 3 well-mixed, 1

decoupled, and 5 stratified PBLs. Figure 17 shows that cloud physical thickness tends to decrease with surface temperature in both the well-mixed and decoupled PBL subsets, but not in the stratified PBL group.

Thus, the observed temperature dependence of low cloud liquid water path and optical thickness over mid-latitude continents is best viewed as a consequence of shifts in the frequency of occurrence of nonconvective versus convective boundary layers. At cooler temperatures, variations in synoptic heat and moisture advection produce a variety of boundary layer types and near-surface RH values and hence a broad distribution of cloud depths and LWP values. As surface temperature rises, the probability of stratified PBLs decreases, convective boundary layers become more common, surface moisture is efficiently mixed upward to produce relatively dry near-surface RH and systematically higher cloud bases, and perhaps more frequent inversions limit the vertical extent of cloud top as well, producing systematically thin low clouds with low LWP. This would

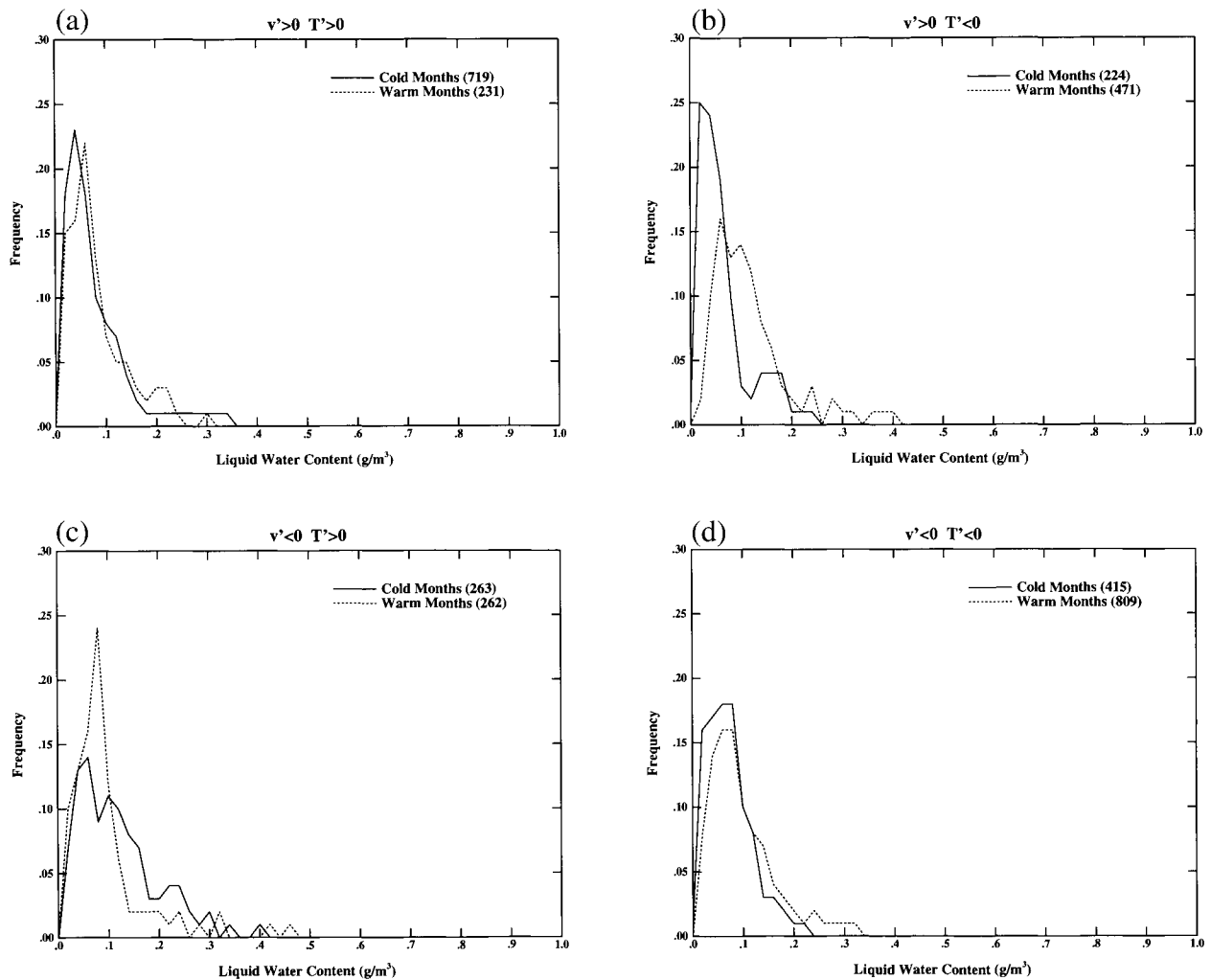


FIG. 10. As in Fig. 8 but for LWC.

explain the nature of the scatter in Fig. 3, which is less suggestive of a continuous variation of LWP with  $T$  and more suggestive of a gradual transition from a broad to a narrow distribution of LWP realizations as  $T$  increases.

Finally, we might ask whether the temperature dependence of low cloud properties is itself simply a function of the degree to which the PBL is decoupled. To crudely assess this, we define a PBL decoupling parameter  $(\Delta q/q) \times 100$  as the percentage specific humidity difference between subcloud and near-cloud-top air (cf. Norris 1998). Figure 18 shows that more strongly decoupled PBLs (to the extent that this parameter captures the phenomenon; large values of the index may also indicate stratified PBLs, which might also be viewed as “decoupled” but not in the same sense as a convective PBL) clearly are associated with lower values of both LWP and LWC. On the other hand, the physically thinnest clouds occur primarily at modest levels of decoupling, and the decoupling parameter itself has no obvious temperature dependence. Thus, the frequency of

occurrence of decoupled (and well-mixed) PBLs, rather than their strength, appears to control the temperature dependence of low cloud properties over midlatitude continents.

## 6. Discussion

### a. Continental versus maritime low-level cloud behavior in the current climate

Continental low clouds have received much less attention in the literature than marine stratus, stratocumulus, and cumulus. Our results show that continental low clouds and associated atmospheric vertical structure exhibit characteristics reminiscent of both midlatitude and subtropical maritime low clouds under different circumstances. For cooler soundings, where the only thick low clouds are observed, the PBL is sometimes highly stratified, RH is high at the surface and above, and there may be no distinct inversion in either  $\theta$  or  $q$  (cf. Figs.

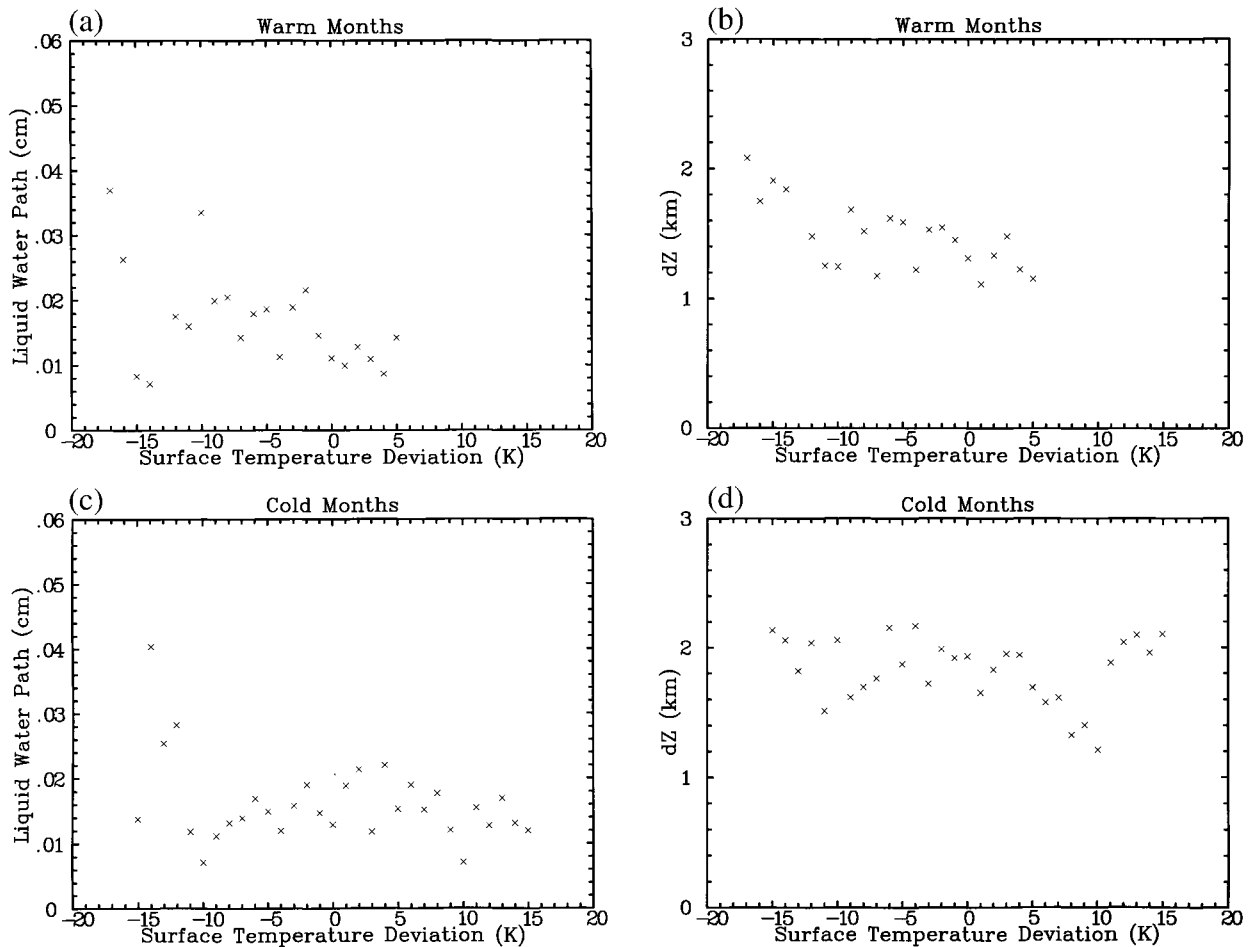


FIG. 11. Low cloud properties binned as a function of instantaneous surface temperature deviation from the seasonal and diurnal cycles in 1-K increments. Warm season (a) LWP and (b) cloud physical thickness. Cold season (c) LWP and (d) cloud physical thickness.

15 and 16). These conditions are reminiscent of those associated with fair- and bad-weather stratus over mid-latitude oceans (cf. Fig. 5 of Norris 1998). Warmer soundings at the SGP, on the other hand, are almost always similar to those characterizing subtropical or midlatitude maritime PBLs under conditions of stratocumulus and/or cumulus (cf. Figs. 1 and 3 of Albrecht et al. 1995; Fig. 3 of Norris 1998). A distinct PBL inversion separates dry, stable free tropospheric air from a convective boundary layer below, either well-mixed or decoupled with multiple convective layers separated by small discontinuities, and RH increases from the surface to the cloud-topped inversion. Thus, much of our understanding of maritime cloudy boundary layers, as well as remaining questions about their formation and decay, can be applied to continental cloudy boundary layers as well.

There are two important differences, however, between the continental and maritime cases. 1) Continental surface RH under warm conditions is much lower than for subtropical-tropical marine boundary layers ( $\sim 60\%$  vs  $\sim 75\%$ ), because of the absence of a constant surface

moisture source and the fast thermal response time of the land surface. Thus, we observe more variability in cloud cover and depth in the continental case, even within the subset of well-mixed and decoupled PBL soundings. 2) Over the ocean, stratocumulus and cumulus tend to occur under cold advection, while fair- and bad-weather stratus usually exist with warm advection (Norris 1998). The opposite is true at the SGP: the mean meridional wind is  $-2 \text{ m s}^{-1}$  for our cold subset (dominated by thick stratus) and  $+4 \text{ m s}^{-1}$  for our warm subset (dominated by stratocumulus and cumulus).

The different behavior can plausibly be attributed to land-ocean differences in the thermodynamic properties of the advected air mass combined with the different thermal response times of the ocean, PBL, and land surface (decreasing from first to last). Maritime PBL RH is high and fairly spatially uniform, so warm air advected over a cold ocean surface will be stable but will cool and easily saturate, especially if accompanied by synoptic lifting. Continental PBL RH is sometimes lower and thus harder to saturate in the absence of vertical mixing. Warm advection over a cooler land surface

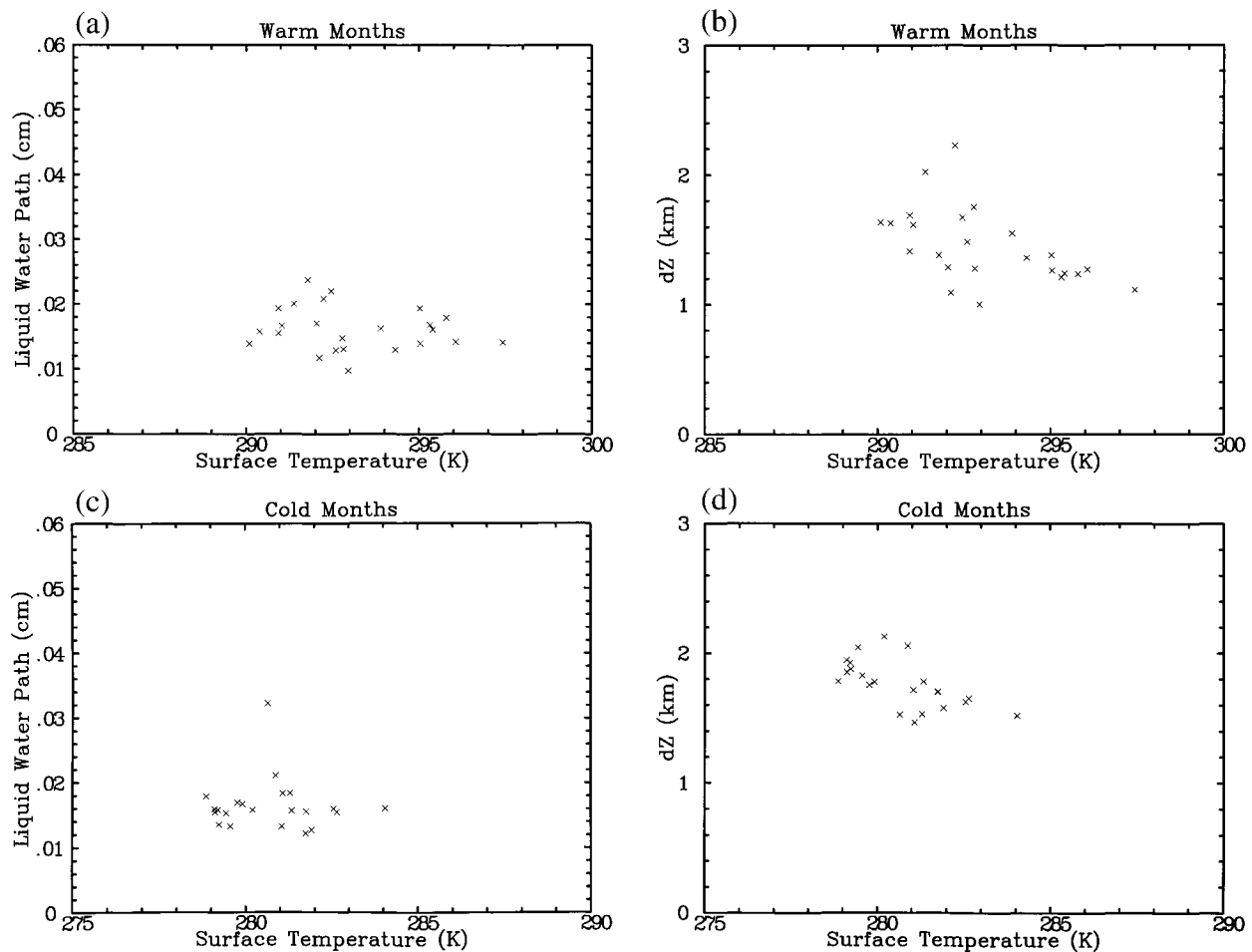


FIG. 12. As in Fig. 11, but for low cloud properties binned by diurnal cycle phase in 1-h increments and plotted vs the mean surface temperature for each diurnal phase.

will warm the surface but have less immediate impact on the air above. If advected from a warm, unstable location, the PBL may already be convective, and if not, diurnal heating of the surface underneath may make it so, promoting a convective cloud-topped PBL with clear air near the ground. Over the ocean, cold advection of air over a warm surface plays the destabilizing role that the diurnal surface response plays over land instead. For cold advection over land, if the advected air mass is moist but stable, contact with the warmer land surface will have little impact on the PBL, but if it is less humid and less stable to begin with, it may be destabilized by the upward sensible heat flux. Thus, we might expect the most variety in low cloud properties under cold advection conditions, which is what we observe at the SGP.

These arguments, of course, are specific to midcontinental locations such as the SGP, where isolated low cloud is prevalent when moderately dry continental air masses are advected over the site. Under conditions of advection from a humid maritime tropical air mass source such as the Gulf of Mexico when the low-level jet is present, the SGP atmosphere destabilizes and deep

convection rather than low cloud dominates. Hence there is no continental equivalent of the persistence of maritime cloudy boundary layers. Likewise, since advection source properties are important for the continental PBL, we expect the SGP behavior to be characteristic of other midcontinental locations but not necessarily indicative of coastal low cloud situations.

#### b. Implications for climate change

Most GCMs with low sensitivity to a doubling of  $\text{CO}_2$  achieve this result because of a negative low cloud optical thickness feedback, because LWC is either prescribed to increase (sometimes adiabatically) with temperature or behaves approximately adiabatically at most temperatures in a prognostic cloud water parameterization while cloud geometrical thickness is fixed. For a midcontinental location and for current climate timescales of variability, at least, our results do not support that behavior in two ways: 1) LWC shows no detectable temperature dependence in either the cold or warm season; 2) Cloud geometric thickness, which also affects

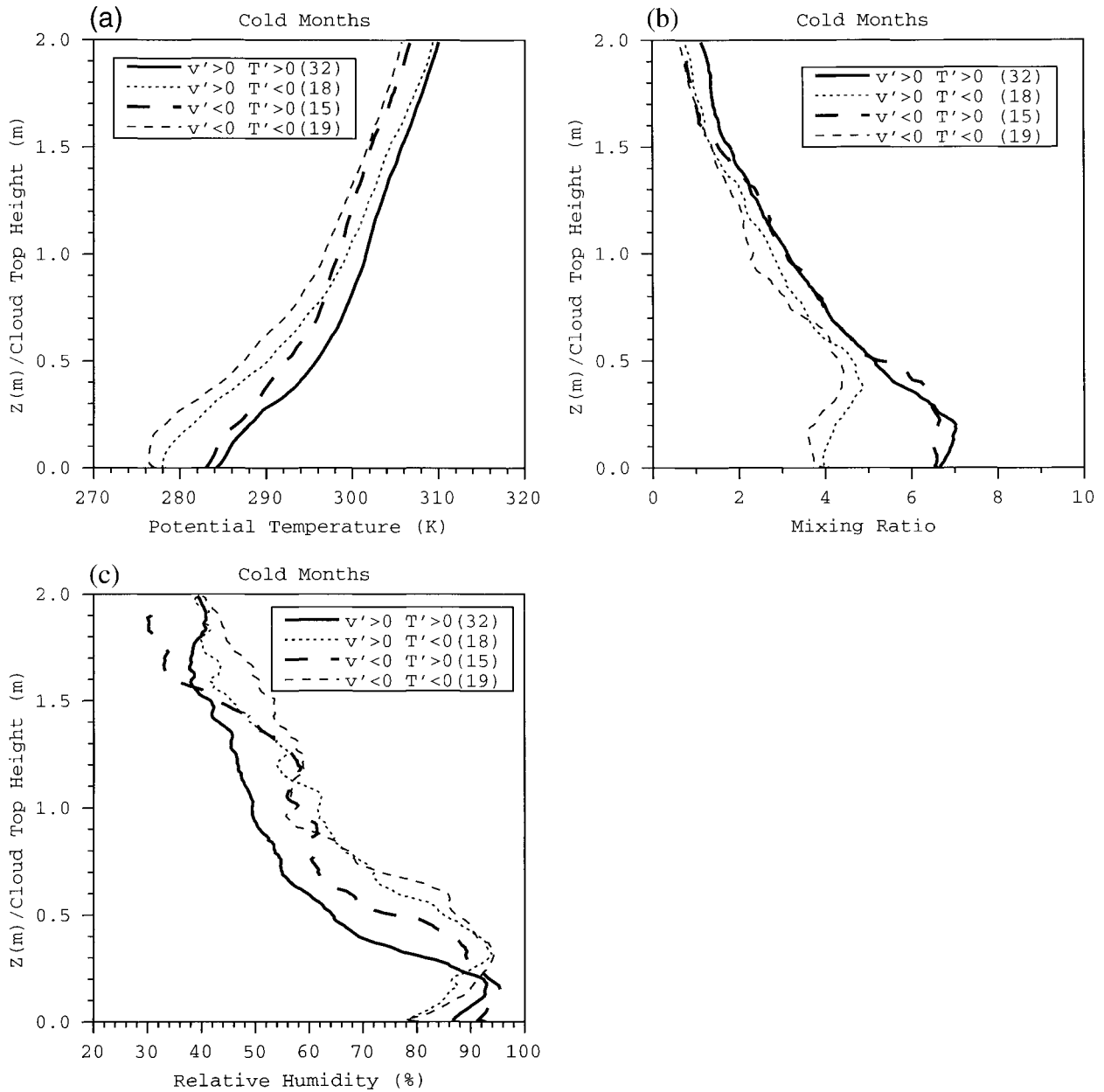


FIG. 13. Composite vertical profiles of (a) potential temperature (K), (b) water vapor mixing ratio ( $\text{g kg}^{-1}$ ), and (c) relative humidity (%) for each synoptic category in the cold season ensemble. Altitude is normalized by the mean of all cloud-top heights observed within  $\pm 1.5$  h of the soundings in each composite. The number of soundings in the composite for each category is indicated in the legend in parentheses.

optical thickness, clearly decreases with temperature in warm environments. The satellite-inferred tendency of low cloud optical thickness and LWP to decrease with  $T$  over much of the world has received less attention than we feel it deserves by modelers because of ambiguities inherent in satellite remote sensing retrievals. Our surface-based analysis reduces such concerns because 1) the effective spatial resolution of our dataset is twice as good as that of the best satellite dataset applied to the problem thus far, reducing the probability that cloud inhomogeneity can completely explain the

result; and 2) more importantly, our ability to isolate specific contributions to the optical thickness variation, and specifically our finding that easily observed and understood variations of cloud-base height with PBL RH account for the dependence over the SGP, addresses the seemingly counterintuitive aspect of the original results.

Our results for the SGP, combined with previous global satellite analyses of low clouds, might be used in two distinct ways to help constrain the low cloud contribution to optical thickness feedback in a climate change.

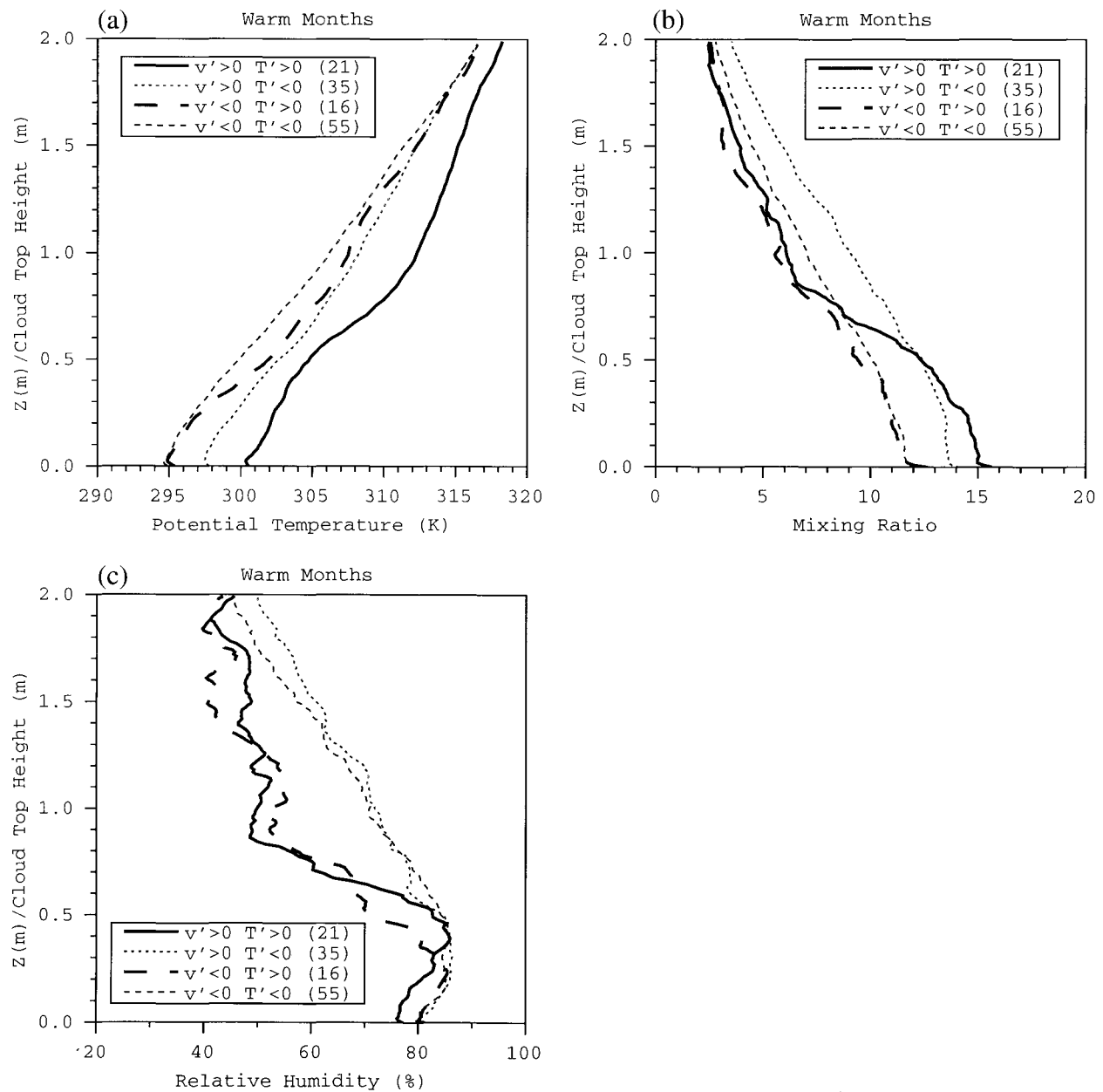


FIG. 14. As in Fig. 13 but for the warm season ensemble.

The first approach uses the data strictly as a validation tool for the GCM's current climate simulation, that is, if a model reproduces the temperature dependence of low cloud optical thickness in the current climate, its prediction of the optical thickness feedback in a climate change should be considered reliable. Tselioudis et al. (1998) have already conducted such a comparison for the GISS GCM. They find that the GCM correctly simulates the transition from  $d\tau/dT > 0$  at high latitudes to  $d\tau/dT < 0$  at low latitudes, although the magnitude of the latter is somewhat overestimated. Furthermore, the  $2 \times \text{CO}_2$  climate change in low cloud  $\tau$ , which

contributes to an overall slightly positive cloud optics feedback (Yao and Del Genio 1999), is similar to the current climate temperature dependence in the model. It would clearly be of interest to know whether the subset of GCMs that predicts negative cloud optics feedback can do so while simultaneously reproducing the current climate  $d\tau/dT < 0$  behavior that characterizes much of the world, including the SGP in summer. Future IPCC assessments should also consider whether it is possible for any GCM to approach the stated  $1.5^\circ\text{C}$  lower limit to climate sensitivity without violating this observational constraint. In addition, although climate

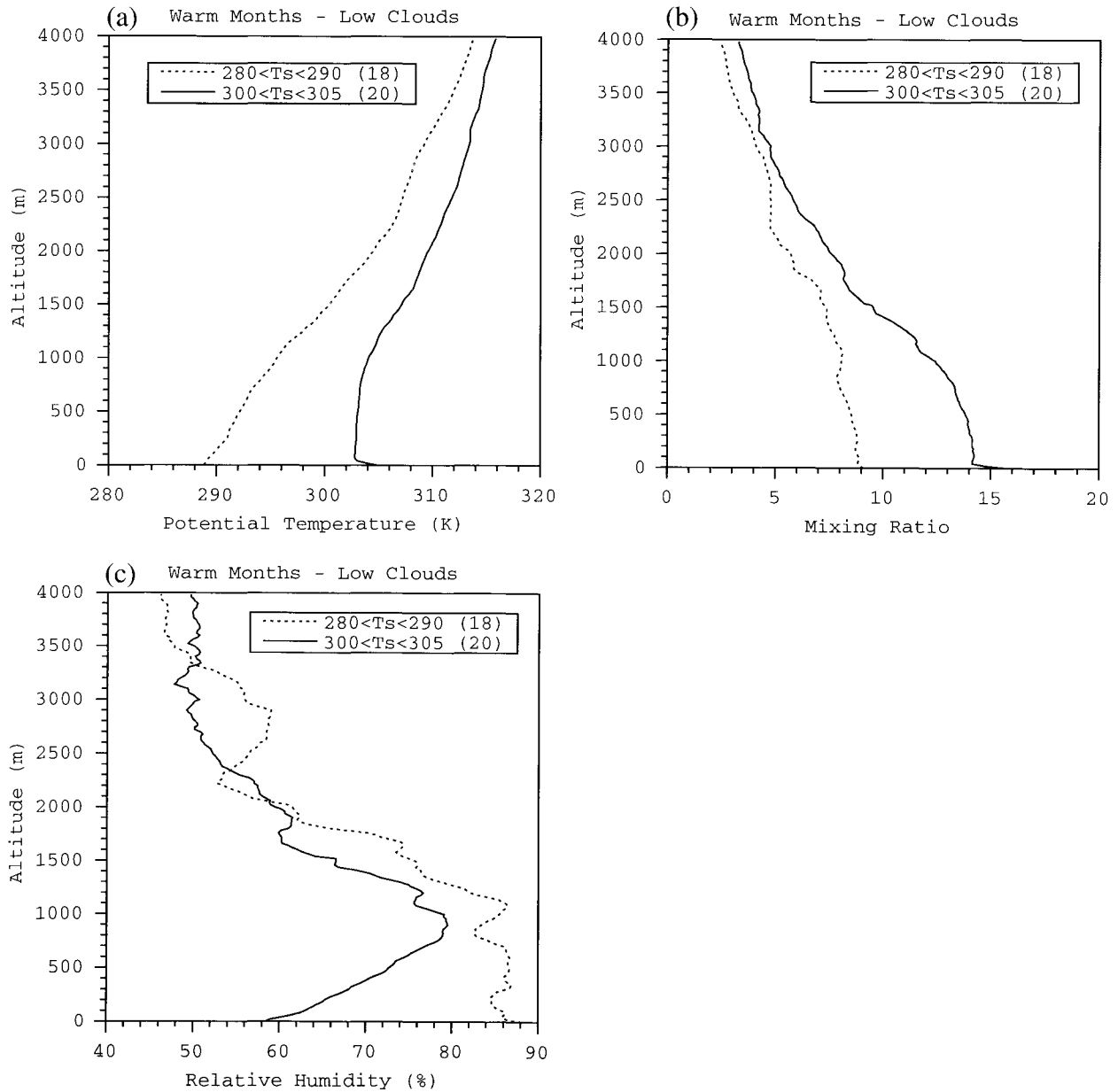


FIG. 15. Composite soundings of (a) potential temperature, (b) mixing ratio, and (c) relative humidity for the warm season ensemble for cold ( $280 < T_s < 290$  K; dotted) and warm ( $300 < T_s < 305$  K; solid) subsets of the population. The number of soundings in each subset is indicated in the legend in parentheses.

models generally predict that the dynamics itself changes little in climate change scenarios, the likelihood that most of the observed LWP variance is dynamics-related suggests this as another important validation target for GCMs. Our segmentation of results by synoptic regime and timescale is one possible way to test models' ability to reproduce the dependence of cloud properties on dynamical state.

One weakness of the above approach is that it does not explicitly address the physical mechanisms that account for the climate change. The GISS GCM partly

but not completely simulates the actual physical mechanisms involved. The cloud parameterization in the GCM relates cloud fraction in three dimensions to RH and stability (Del Genio et al. 1996), so that as RH decreases, both the areal extent and physical thickness of the cloud decrease. This is exactly the behavior we observe at the SGP (Fig. 5). The GCM's LWC also does not increase with temperature in midlatitudes (Tselioudis et al. 1998), consistent with the behavior of the ARM data. On the other hand, the coarse vertical resolution of that version of the model is inadequate to capture the

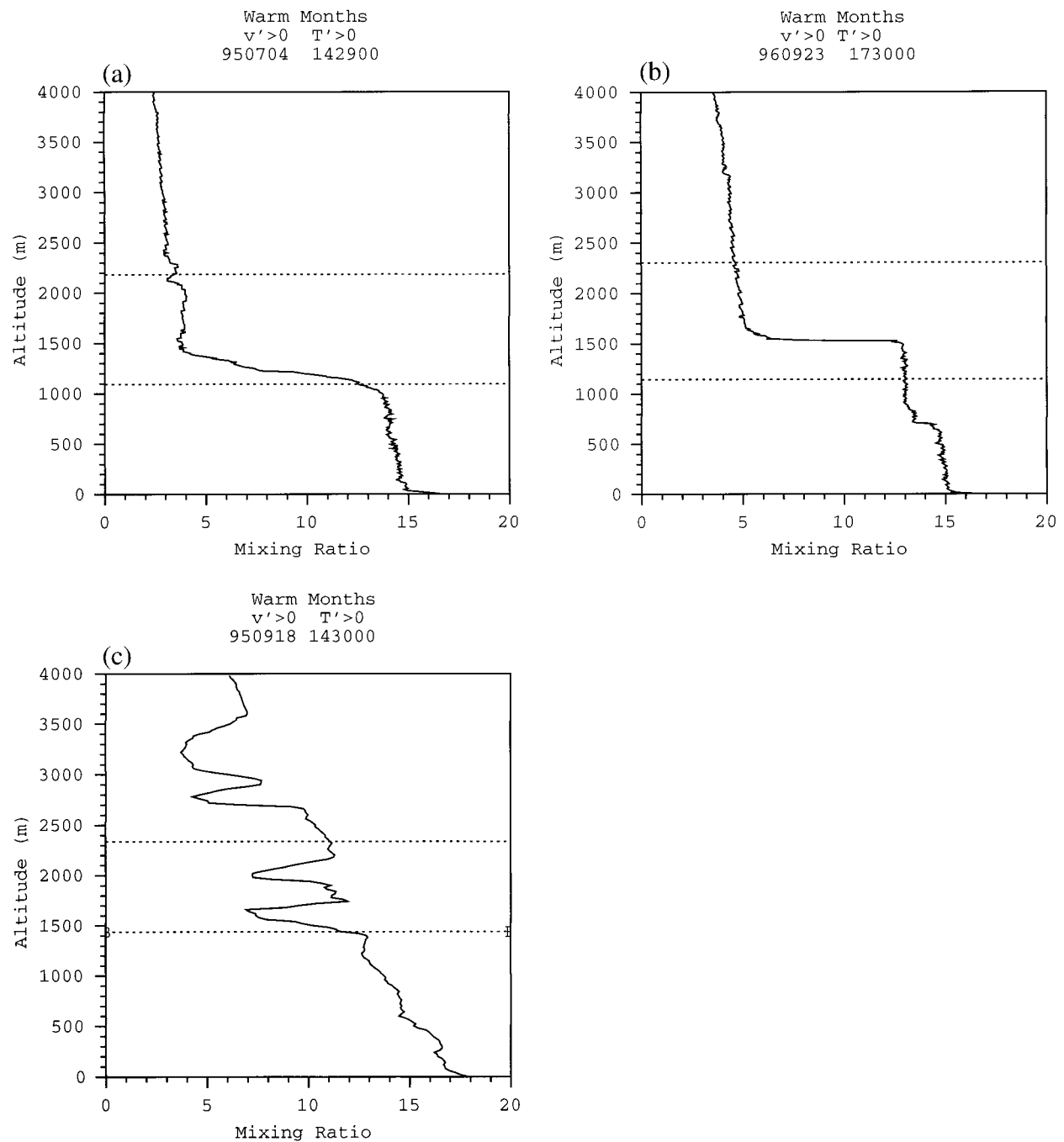


FIG. 16. Examples of (a) well-mixed (1429:00 UTC 4 Jul 1995) (b) decoupled (1730:00 UTC 23 Sep 1996), and (c) stratified (1430:00 UTC 18 Sep 1995) PBL humidity profiles in the warm season ensemble, each occurring in the  $v' > 0$ ,  $T' > 0$  synoptic category. The mean cloud base and height within  $\pm 1.5$  h of each sounding is indicated by the horizontal dotted lines.

detailed structure of PBL inversions and decoupled boundary layers, so confirmation of the result with a higher vertical resolution model would be desirable. Figure 4 suggests that  $\Delta z$  should decrease by several hundred meters in a  $2 \times \text{CO}_2$  climate change. Thus, unless higher vertical resolution than this can be achieved, GCMs must consider parameterizing cloud

fraction in the vertical as well as the horizontal. Additional variance in LWP associated with subgrid-scale vertical velocity fluctuations is not yet incorporated in the GISS GCM but may be important in simulating frequency distributions such as those portrayed in Figs. 8–10. Over subtropical oceans, where the satellite data also indicate  $d\tau/dT < 0$ , surface RH and thus cloud-

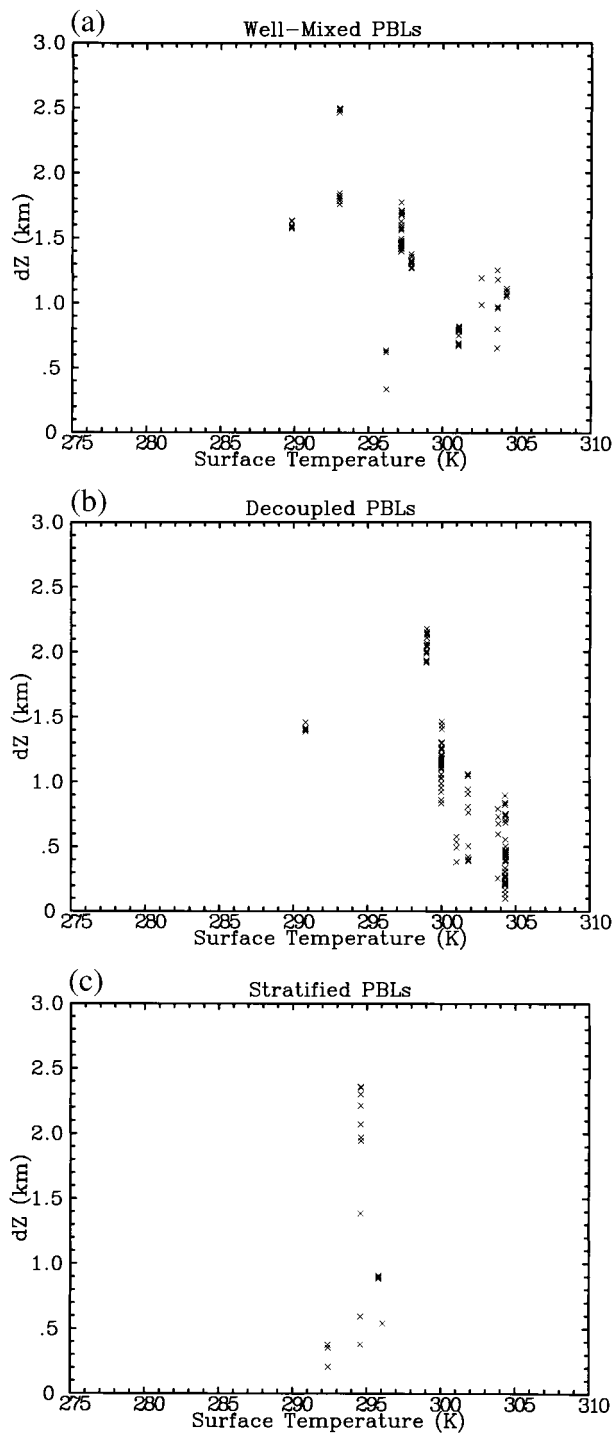


FIG. 17. Cloud physical thickness vs surface temperature for the warm subset of the warm season ensemble for conditions of (a) well-mixed, (b) decoupled, and (c) stratified PBLs.

base height may not respond to sea surface temperature changes in the same way as continental clouds do (cf. Albrecht et al. 1995), so other mechanisms may need to be invoked. Finally, over tropical oceans the GCM behavior is clearly explained by a different mechanism,

the depletion of liquid water by entrainment and drizzle; these mechanisms have not yet been validated against observations.

Alternatively, can we use the observations directly to infer the sense of low cloud optics feedback without resorting to models at all? Our finding that low clouds tend to thin with warming on three different timescales (diurnal, synoptic, seasonal) argues that the behavior we observe is general in nature. However, the best analogy to the combination of intrinsic temperature dependence and dynamics effects expected in a climate change is the seasonal cycle. If we assume that greenhouse climate change will be characterized by an increase in temperature combined with a decrease in meridional temperature gradient (the latter due to polar amplification associated with sea-ice-albedo feedback and the absence of convection at high latitudes), then the winter-to-summer variation in baroclinic wave activity may provide a suitable proxy for *midlatitude* aspects of long-term climate change. From Table 2 we see that the warm sector and building high pressure regions of midlatitude weather systems (i.e., areas with  $T' > 0$ ) are those in which LWP decreases from winter to summer, while the  $T' < 0$  sectors experience an increase or no change in LWP. Averaged over all observations, low cloud LWP is seasonally invariant at the SGP, with winter-to-summer increases in LWC being offset by physical thinning of clouds. (Partly, this seasonal invariance occurs because low clouds occur less frequently in  $T' > 0$  situations in summer but more frequently in  $T' < 0$  situations.) Together, these features appear to be consistent with Tselioudis and Rossow's (1994) impression of midlatitude continents as transitional regions between higher latitude areas of negative cloud optics feedback and lower latitude areas of positive cloud optics feedback. The fact that LWP and  $\Delta z$  decrease with temperature on shorter timescales preferentially in the warm season (Figs. 3, 4, 11) suggests that positive low cloud optics feedback over midlatitude continents might be primarily a summer phenomenon, when temperatures are warm enough for the climate change to significantly increase the frequency of convective PBLs and decrease the occurrence of stratified PBLs. This, combined with the greater insolation available in summer, strengthens the argument for a net positive low cloud optics feedback at these latitudes.

If cloud physical thickness variation associated with boundary layer structure variation is indeed the principal control on low cloud optical thickness over midlatitude continents, then our results may imply a positive low cloud *cover* feedback in these regions as well. Assuming a Gaussian distribution of LCLs in a convective PBL topped by an inversion, Considine et al. (1997) relate the shape of the probability distribution of LWP to the cloud fraction, the latter determined as the fraction of surface parcels that have LCLs beneath the inversion. If clouds thin with warming because surface RH decreases and LCL increases, as is the case at the SGP,

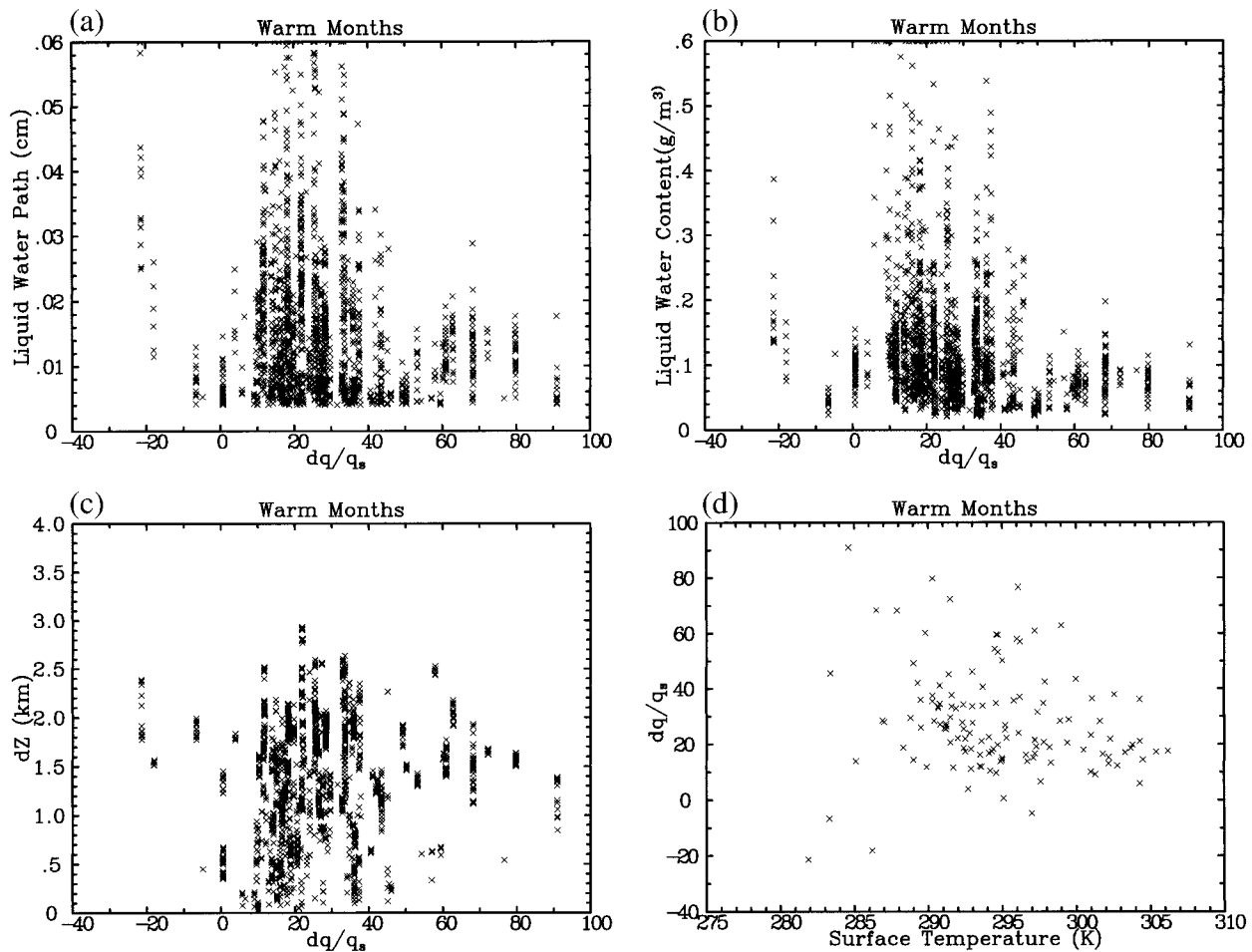


FIG. 18. Effect of PBL decoupling on warm season low cloud properties. (a) LWP vs decoupling parameter. (b) LWC vs decoupling parameter. (c) Cloud physical thickness vs decoupling parameter. (d) Decoupling parameter vs surface temperature.

then the probability of parcels reaching the inversion without saturating increases, and thus the cloud cover decreases. Our very limited sample of soundings with WMO cloud classifications is consistent with this—cloud cover is lower for the warm subset than for the cool subset. Yao and Del Genio (1999) find that mid-latitude continents are a transition location between increasing cloud cover at higher latitudes, and decreasing cloud cover at lower latitudes, in a  $2 \times CO_2$  warming (their Fig. 8), consistent with our impression of these latitudes as a transitional region for low cloud optics feedback.

We note that our conclusions apply only to the role of *low* clouds in climate change. Middle and high clouds, which are not directly coupled to the surface, may be governed by different physics, and there is as yet no observational or theoretical basis for predicting the sign of their contributions to cloud optics feedback. In the GISS GCM, for example, increased condensate detrainment into cumulus anvils in a warm climate produces a negative shortwave component of cloud optics

feedback for this cloud type, which approximately cancels the positive shortwave feedback due to decreasing low cloud  $\tau$  (Yao and Del Genio 1999). The net positive cloud optics feedback in the GCM is then caused by the increased longwave emissivity of thinner high clouds in the warmer climate. The resulting global sensitivity of  $3.1^\circ C$  in that model is a compromise between the high sensitivity that would occur if all clouds behaved like the low-latitude and midlatitude low clouds in the model, and the very low sensitivity that would occur if the cloud optics feedback were not positive in some parts of the world for some cloud types. A very low global sensitivity is unlikely to be realized unless cloud optics feedback is negative almost everywhere; our ARM results combined with the previous ISCCP and SSM/I analyses suggest that this is not the case in the real world.

To solidify our conclusions, several types of observations are needed. Coincident cloud-top and cloud-base information, and thus more accurate LWC estimates, can in principle come from the millimeter cloud radar

(MMCR) at the SGP, but only if the spurious low-altitude signal that plagues the instrument in summer (Moran et al. 1998) can be eliminated. Droplet effective radius retrievals from the MMCR would complete the list of individual contributions to optical thickness, and cloud optical thickness itself can potentially be retrieved from several surface-based instruments at the SGP, but is not yet being provided as a routine ARM product. Our study has been limited to low clouds with  $\tau \geq 5$  because of the limitations of the MWR LWP retrieval. Improvements in the algorithm that better account for the dry air contribution to the microwave signal will allow the analysis to be extended to optically thinner clouds, and accounting for the dependence of liquid water emission on cloud temperature will reduce LWP errors for the clouds we already detect (J. Liljegren 1998, personal communication). However, thin low clouds contribute only about one-third of the shortwave forcing of all low clouds (Chen et al. 2000), and our results are consistent with Tselioudis and Rossow (1994), whose analysis includes thinner clouds, so we do not expect thin low clouds to qualitatively alter our conclusions. An analogous study for low clouds at the ARM tropical west Pacific sites at Manus and Nauru islands would also be of considerable interest, given the GISS GCM's prediction of low cloud optical thickness limitation by LWC sinks rather than physical thickness changes at these latitudes. However, the combination of existing satellite and surface remote sensing evidence discussed in this paper already appears to invalidate the assumption of global negative low cloud optics feedback made by many workers in the field.

**Acknowledgments.** The authors thank G. Tselioudis, W. Rossow, T. Charlock, J. Liljegren, and R. Somerville for helpful discussions on this topic. This work was supported by the DOE Atmospheric Radiation Measurement program.

#### REFERENCES

- Albrecht, B. A., M. P. Jensen, and W. J. Syrett, 1995: Marine boundary layer structure and fractional cloudiness. *J. Geophys. Res.*, **100**, 14 209–14 222.
- Betts, A. K., and Harshvardhan, 1987: Thermodynamic constraint on the cloud liquid water feedback in climate models. *J. Geophys. Res.*, **92**, 8483–8485.
- Cess, R. D., and Coauthors, 1990: Intercomparison and interpretation of climate feedback processes in 19 atmospheric general circulation models. *J. Geophys. Res.*, **95**, 16 601–16 615.
- Charlock, T. P., 1982: Cloud optical feedback and climate stability in a radiative-convective model. *Tellus*, **34**, 245–254.
- Chen, T., W. B. Rossow, and Y. Zhang, 2000: Radiative effects of cloud-type variations. *J. Climate*, **13**, 264–286.
- Considine, G., J. A. Curry, and B. Wielicki, 1997: Modeling cloud fraction and horizontal variability in marine boundary layer clouds. *J. Geophys. Res.*, **102**, 13 517–13 525.
- Curry, J. A., C. D. Ardeel, and L. Tian, 1990: Liquid water content and precipitation characteristics of stratiform clouds as inferred from satellite microwave measurements. *J. Geophys. Res.*, **95**, 16 659–16 671.
- Deardorff, J. W., 1980: Cloud-top entrainment instability. *J. Atmos. Sci.*, **37**, 131–147.
- Del Genio, A. D., M.-S. Yao, W. Kovari, and K. K.-W. Lo, 1996: A prognostic cloud water parameterization for global climate models. *J. Climate*, **9**, 270–304.
- Feigelson, E. M., 1978: Preliminary radiation model of a cloudy atmosphere. Part I: Structure of clouds and solar radiation. *Beitr. Phys. Atmos.*, **51**, 203–229.
- Greenwald, T. J., G. L. Stephens, S. A. Christopher, and T. H. Vonder Haar, 1995: Observations of the global characteristics and regional radiative effects of marine cloud liquid water. *J. Climate*, **8**, 2928–2946.
- Houghton, J. T., L. G. Meira Filho, B. A. Callander, N. Harris, A. Kattenberg, and K. Maskell, Eds., 1996: *Climate Change 1995: The Science of Climate Change*. Cambridge University Press, 572 pp.
- Lau, N.-C., and M. W. Crane, 1995: A satellite view of the synoptic-scale organization of cloud properties in midlatitude and tropical circulation systems. *Mon. Wea. Rev.*, **123**, 1984–2006.
- Li, Z.-X., and H. LeTreut, 1992: Cloud-radiation feedbacks in a general circulation model and their dependence on cloud modeling assumptions. *Climate Dyn.*, **7**, 133–139.
- Lin, B., and W. B. Rossow, 1994: Observations of cloud liquid water path over oceans: Optical and microwave remote sensing methods. *J. Geophys. Res.*, **99**, 20 909–20 927.
- MacVean, M. K., and P. J. Mason, 1990: Cloud-top entrainment instability through small-scale mixing and its parameterization in numerical models. *J. Atmos. Sci.*, **47**, 1012–1030.
- Moran, K. P., B. E. Martner, M. J. Post, R. A. Kropfli, D. C. Welsh, and K. B. Widener, 1998: An unattended cloud-profiling radar for use in climate research. *Bull. Amer. Meteor. Soc.*, **79**, 443–455.
- Norris, J. R., 1998: Low cloud type over the ocean from surface observations. Part I: Relationship to surface meteorology and the vertical distribution of temperature and moisture. *J. Climate*, **11**, 369–382.
- Paltridge, G. W., 1980: Cloud-radiation feedback to climate. *Quart. J. Roy. Meteor. Soc.*, **106**, 895–899.
- Phillips, T. J., 1994: A summary documentation of the AMIP models. Program for Climate Model Diagnosis and Intercomparison Rep. 18 (UCRL-ID-116384), University of California, Lawrence Livermore National Laboratory, Livermore, CA, 343 pp. [Available from PCMDI, P.O. Box 808, Livermore, CA 94551.]
- Randall, D. A., 1980: Conditional instability of the first kind upside-down. *J. Atmos. Sci.*, **37**, 125–130.
- , 1984: Stratocumulus cloud deepening through entrainment. *Tellus*, **36A**, 446–457.
- Roeckner, E., 1988: Cloud-radiation feedbacks in a climate model. *Atmos. Res.*, **21**, 293–303.
- Senior, C. A., and J. F. B. Mitchell, 1993: Carbon dioxide and climate: The impact of cloud parameterization. *J. Climate*, **6**, 393–418.
- Somerville, R. C. J., and L. A. Remer, 1984: Cloud optical thickness feedbacks in the CO<sub>2</sub> climate problem. *J. Geophys. Res.*, **89**, 9668–9672.
- Tselioudis, G., and W. B. Rossow, 1994: Global, multiyear variations of optical thickness with temperature in low and cirrus clouds. *Geophys. Res. Lett.*, **21**, 2211–2214.
- , —, and D. Rind, 1992: Global patterns of cloud optical thickness variation with temperature. *J. Climate*, **5**, 1484–1495.
- , A. D. Del Genio, W. Kovari Jr., and M.-S. Yao, 1998: Temperature dependence of low cloud optical thickness in the GISS GCM: Contributing mechanisms and climate implications. *J. Climate*, **11**, 3268–3281.
- U.S. National Academy of Sciences, 1979: *Carbon Dioxide and Climate: A Scientific Assessment*. U.S. National Academy of Sciences, 22 pp.
- Yao, M.-S., and A. D. Del Genio, 1999: Effects of cloud parameterization on the simulation of climate changes in the GISS GCM. *J. Climate*, **12**, 761–779.